2018 Outfall Benthic Monitoring Results

Massachusetts Water Resources Authority
Environmental Quality Department
Report 2019-06

Citation:

Rutecki DA, Diaz RJ, Nestler EC, Codiga DL, Madray ME. 2019. **2018 Outfall Benthic Monitoring Results**. Boston: Massachusetts Water Resources Authority. Report 2019-06. 59 p.

Cover photograph credit: Chris Baker, Normandeau Associates

Environmental Quality Department reports can be downloaded from
http://www.mwra.com/harbor/enquad/trlist.html

2018 Outfall Benthic Monitoring Results

Submitted to

Massachusetts Water Resources Authority
Environmental Quality Department
100 First Avenue
Charlestown Navy Yard
Boston, MA 02129
(617) 242-6000

Prepared by

Deborah A Rutecki[1]
Robert J. Diaz[2]
Eric C.Nestler[1]
Daniel L. Codiga[3]
Maureen E. Madray[1]

[1]Normandeau Associates, Inc.
25 Nashua Road
Bedford, NH 30110

[2]Diaz and Daughters
6198 Driftwood Lane
Ware Neck, VA 23178

[3]Massachusetts Water Resources Authority
Boston, MA 02129

September 2019

Environmental Quality Report No. 2019-06

TABLE OF CONTENTS

PAGE

FIGURES

PAGE

TABLES

PAGE

EXECUTIVE SUMMARY

The Massachusetts Water Resources Authority (MWRA) has conducted long-term monitoring since 1992 in Massachusetts Bay and Cape Cod Bay to evaluate the potential effects of discharging secondary treated effluent 15 kilometers (km) offshore in Massachusetts Bay. Relocation of the outfall from Boston Harbor to Massachusetts Bay in September 2000 raised concerns about potential effects of the discharge on the offshore benthic (bottom) environment, which are addressed by the results reported here.

Benthic monitoring during 2018 included soft-bottom sampling for sediments and infauna at 14 nearfield and farfield stations, and sediment profile imaging (SPI) at 23 nearfield stations.

Sediment conditions were characterized based on spore counts of the anaerobic bacterium, *Clostridium perfringens*, analyses of sediment grain size composition and total organic carbon (TOC). *C. perfringens* concentrations during 2018 were highest at sites closest to the discharge. These findings are consistent with those obtained since outfall relocation (e.g. Nestler et al. 2018, Maciolek et al. 2007, 2008). The results for *C. perfringens*, therefore, provide a sensitive "effluent signature", or evidence of low levels of settlement of solids from the effluent at sites in close proximity (within 2 km) to the outfall. Neither sediment grain size nor TOC have exhibited appreciable changes from the baseline period and this pattern continued in 2018. These results indicate the only detectable influence of the wastewater discharge on sediment conditions is seen in *Clostridium* spores, consistent with prior monitoring results (Nestler et al. 2018, Nestler et al. 2017, Maciolek et al. 2008).

As seen in previous years, there was no evidence of impacts to the infaunal communities in Massachusetts Bay from the offshore outfall in 2018. Monitoring results have consistently suggested that deposition of particulate organic matter from the wastewater discharge is not occurring at levels that disturb or smother animals near the outfall. There were no Contingency Plan threshold exceedances for any infaunal diversity measures in 2018. Multivariate analyses indicated that patterns in the distribution of faunal assemblages reflect habitat types at the sampling stations. Infaunal data in 2018 continue to suggest that the macrobenthic communities at sampling stations near the outfall have not been adversely impacted by the wastewater discharge.

The 2018 SPI survey found no indication that the wastewater discharge has resulted in low levels of dissolved oxygen in nearfield sediments. The average thickness of the sediment oxic layer in 2018 was greater than during the baseline period and among the highest reported during post-discharge years. These results support previous findings that organic loading and an associated decrease in oxygen levels have not been a problem at the nearfield benthic monitoring stations (Nestler et al. 2018, Maciolek et al. 2008).

This report includes an assessment of regional storminess during sediment monitoring that began in 1992, and tests whether there is evidence that storms are impacting the benthos. This assessment strongly supports that the trend seen in the SPI results likely results from the coarsening of sediment grain-size caused by sediment mixing and transport associated with storms that produced a decline in visible biogenic structures in the images.

The outfall is located in an area dominated by hydrodynamic and physical factors, including tidal and storm currents, turbulence, and sediment transport (Butman et al. 2008). These physical factors, combined with the high quality of the effluent discharged into the Bay (Taylor 2010), are the principal reasons that benthic habitat quality has remained high in the nearfield area.

1 INTRODUCTION

The Massachusetts Water Resources Authority (MWRA) has conducted long-term monitoring since 1992 in Massachusetts Bay and Cape Cod Bay to evaluate the potential effects of discharging secondary treated effluent 15 kilometers (km) offshore in Massachusetts Bay. Relocation of the outfall from Boston Harbor to Massachusetts Bay in September 2000 raised concerns about potential effects of the discharge on the offshore benthic (bottom) environment. These concerns focused on three issues: (1) eutrophication and related low levels of dissolved oxygen; (2) accumulation of toxic contaminants in depositional areas; and (3) smothering of animals by particulate matter.

Under its Ambient Monitoring Plan (MWRA 1991, 1997, 2001, 2004, 2010) the MWRA has collected extensive information over a nine-year baseline period (1992–2000) and an eighteen-year post-diversion period (2001–2018). These studies include surveys of sediments and soft-bottom communities using traditional grab sampling and sediment profile imaging (SPI) as well as surveys of hard-bottom communities using a remotely operated vehicle (ROV). Data collected by this program allow for a more complete understanding of the bay system and provide a basis to explain any changes in benthic conditions and to address the question of whether MWRA's discharge has contributed to any such changes.

Benthic monitoring during 2018 was conducted following the current Ambient Monitoring Plan (MWRA 2010) which is required under MWRA's effluent discharge permit for the Deer Island Treatment Plant. Under this plan, annual monitoring includes soft-bottom sampling for sediment conditions and infauna at 14 nearfield and farfield stations, and Sediment Profile Imaging (SPI) at 23 nearfield stations. Every third year, sediment contaminants are evaluated (at the same 14 stations where infauna and sediment condition samples are collected) and hard-bottom surveys are conducted (at 23 nearfield stations). The most recent sediment contaminant monitoring and hard-bottom surveys were conducted in 2017 (next sampling will be in 2020). Sediment contaminant monitoring in 2017 found no indication that toxic contaminants from the wastewater discharge are accumulating in depositional areas surrounding the outfall (Nestler et al. 2018). Monitoring results for 2017 also indicated that hard-bottom benthic communities near the outfall have not changed substantially during the post-diversion period as compared to the baseline period (Nestler et al. 2018).

This report summarizes key findings from the 2018 benthic surveys, with a focus on the most noteworthy observations relevant to understanding the potential effects of the discharge on the offshore benthic environment. Results of 2018 benthic monitoring were presented at MWRA's Annual Technical Workshop on April 4, 2019. This report builds on the presentations and discussions at that meeting.

2 METHODS

Methods used to collect, analyze, and evaluate all sample types remain largely consistent with those reported for previous monitoring years (Nestler et al. 2018, Maciolek et al. 2008). Detailed descriptions of the methods are contained in the Quality Assurance Project Plan (QAPP) for Benthic Monitoring 2017–2020 (Rutecki et al. 2017). A brief overview of methods, focused on information that is not included in the QAPP, is provided in Sections 2.1 to 2.3.

2.1 FIELD METHODS

Sediment and infauna sampling was conducted at 14 stations on August 2, 2018 (Figure 2-1). To aid in analyses of potential spatial patterns reported herein, these stations are grouped, based on distance from the discharge, into four "monitoring areas" within Massachusetts Bay[1]:

- Nearfield stations NF13, NF14, NF17, and NF24, located in close proximity (less than 2 km) to the offshore outfall
- Nearfield stations NF04, NF10, NF12, NF20, NF21, and NF22, located in Massachusetts Bay but farther than 2 km (and less than 5 km) from the offshore outfall
- Transition area station FF12, located between Boston Harbor and the offshore outfall (just less than 8 km from the offshore outfall)
- Farfield reference stations FF01A, FF04, and FF09, located in Massachusetts Bay but farther than 13 km from the offshore outfall

Sampling effort at these stations has varied somewhat during the monitoring program. In particular, from 2004-2010 some stations were sampled only during even years (NF22, FF04 and FF09), Stations NF17 and NF12 were sampled each year, and the remaining stations were sampled only during odd years.

Sampling at Station FF04 within the Stellwagen Bank National Marine Sanctuary was conducted in accordance with Research Permit SBNMS-2016-003.

Soft-bottom stations were sampled for grain size composition, total organic carbon (TOC), and the sewage tracer *Clostridium perfringens*. Infauna samples were also collected using a 0.04-m^2 Ted Young-modified van Veen grab, and were rinsed with filtered seawater through a 300-µm-mesh sieve.

Sediment Profile Imaging (SPI) samples were collected in triplicate at 23 nearfield stations on August 6, 2018 (Figure 2-2).

[1] The current monitoring areas form a subset of stations that were sampled before 2011. For example, the transition area formerly included station FF12 and two others that are no longer sampled.

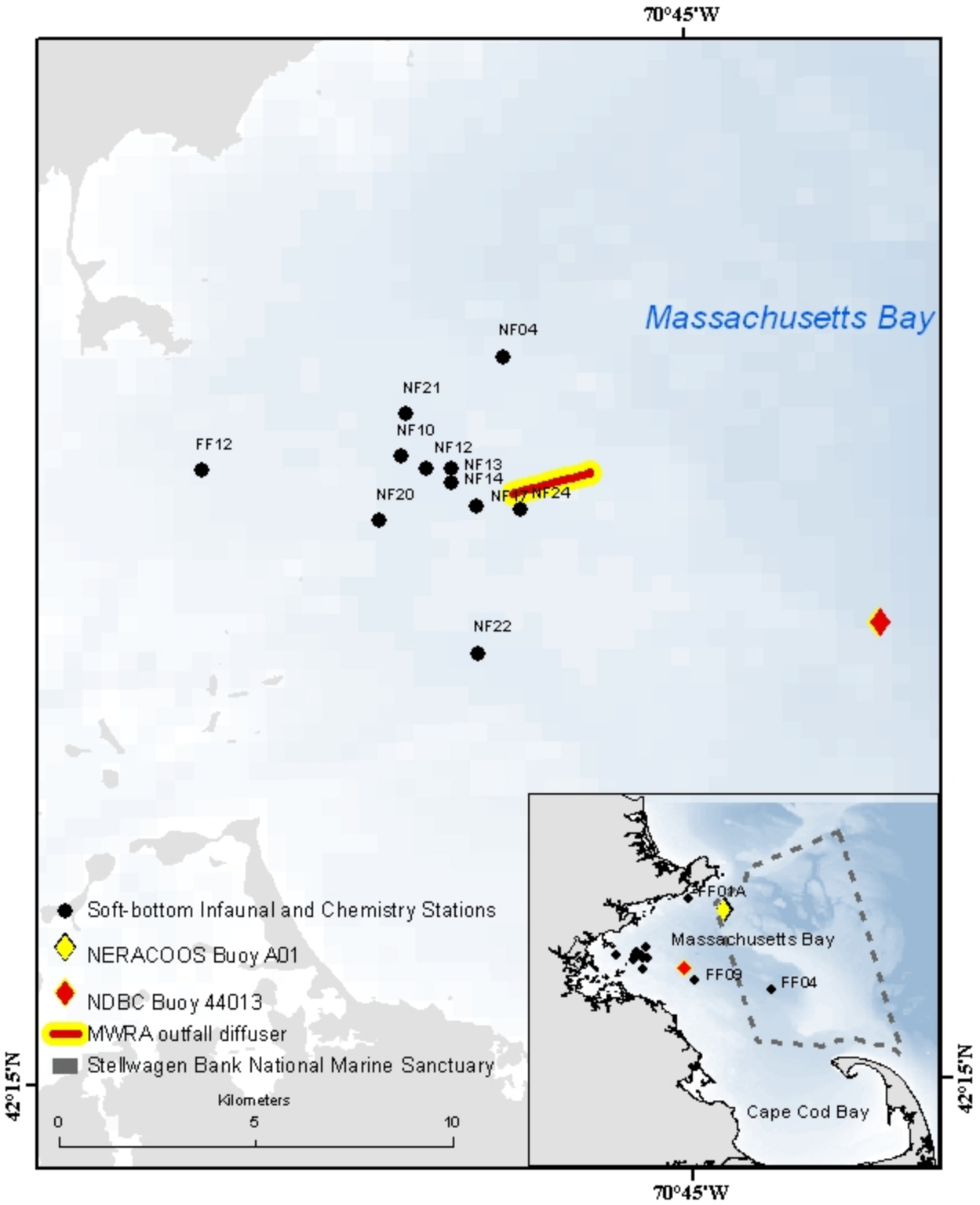

Figure 2-1. Locations of soft-bottom sampling stations for 2018.

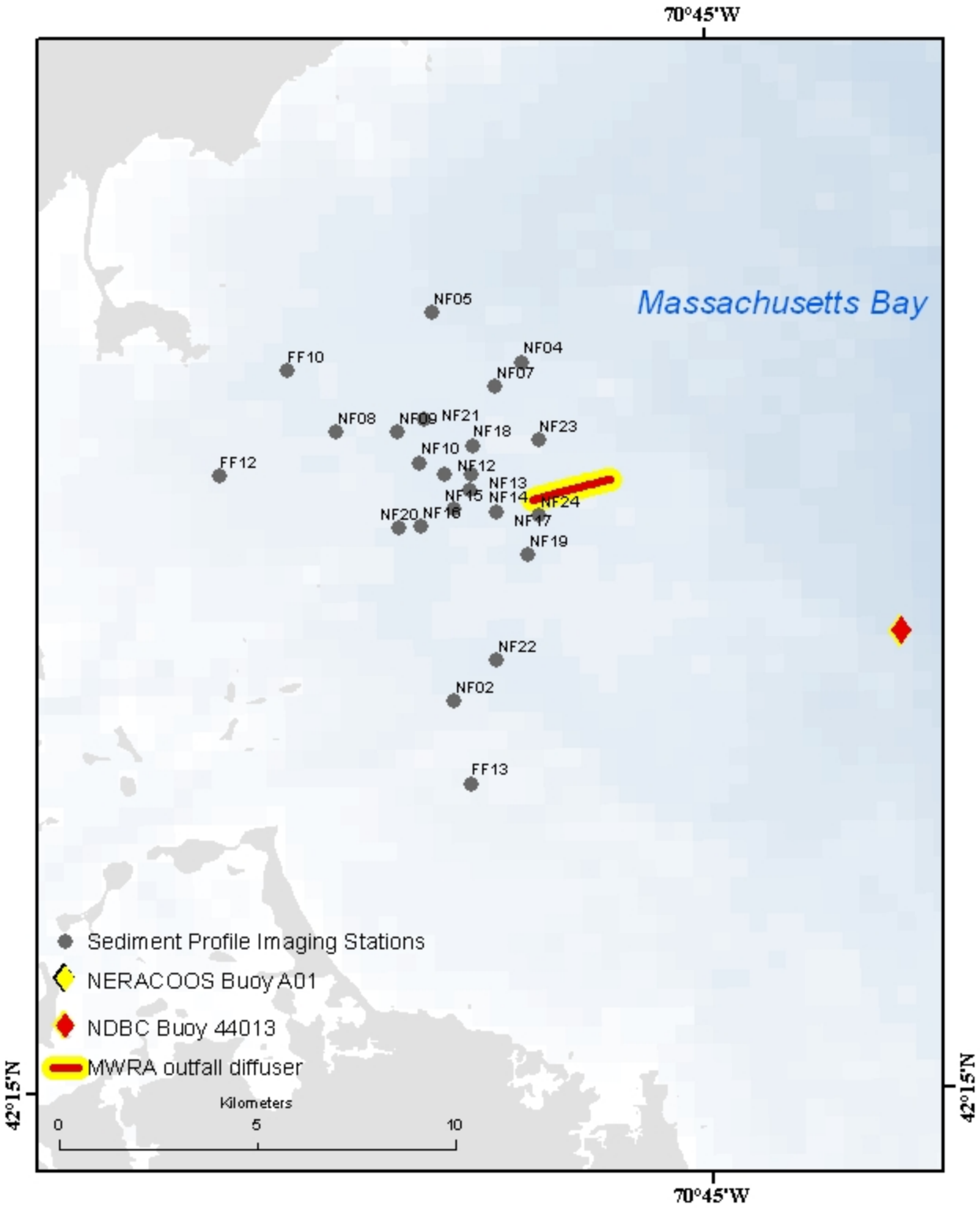

Figure 2-2. Locations of sediment profile imaging stations for 2018.

2.2 LABORATORY METHODS

All bacteriological, physical and chemical analyses were conducted by MWRA's DLS Laboratory following the procedures described in Constantino et al. (2014). All sample processing, including sorting, identification, and enumeration of infaunal organisms, was done following methods consistent with the QAPP (Rutecki et al. 2017).

2.3 DATA HANDLING, REDUCTION, AND ANALYSIS

All benthic data were extracted directly from the HOM database and imported into Excel. Data handling, reduction, graphical presentations and statistical analyses were performed as described in the QAPP (Rutecki et al. 2017) or by Maciolek et al. (2008).

Additional multivariate techniques were used to evaluate infaunal communities. Multivariate analyses were performed using PRIMER v6 (Plymouth Routines in Multivariate Ecological Research) software to examine spatial patterns in the overall similarity of benthic assemblages in the survey area (Clarke 1993, Warwick 1993, Clarke and Green 1988). These analyses included classification (cluster analysis) by hierarchical agglomerative clustering with group average linking and ordination by non-metric multidimensional scaling (MDS). Bray-Curtis similarity was used as the basis for both classification and ordination. Prior to analyses, infaunal abundance data were fourth-root transformed to ensure that all taxa, not just the numerical dominants, would contribute to similarity measures.

Cluster analysis produces a dendrogram that represents discrete groupings of samples along a scale of similarity. This representation is most useful when delineating among sites with distinct community structure. MDS ordination produces a plot or "map" in which the distance between samples represents their rank ordered similarities, with closer proximity in the plot representing higher similarity. Ordination provides a more useful representation of patterns in community structure when assemblages vary along a steady gradation of differences among sites. Stress provides a measure of adequacy of the representation of similarities in the MDS ordination plot (Clarke 1993). Stress levels less than 0.05 indicate an excellent representation of relative similarities among samples with no prospect of misinterpretation. Stress less than 0.1 corresponds to a good ordination with no real prospect of a misleading interpretation. Stress less than 0.2 still provides a potentially useful two-dimensional picture, while stress greater than 0.3 indicates that points on the plot are close to being arbitrarily placed. Together, cluster analysis and MDS ordination provide a highly informative representation of patterns of community-level similarity among samples. The "similarity profile test" (SIMPROF) was used to provide statistical support for the identification of faunal assemblages (i.e., selection of cluster groups). SIMPROF is a permutation test of the null hypothesis that the groups identified by cluster analysis (samples included under each node in the dendrogram) do not differ from each other in multivariate structure.

To help with assessment of spatial patterns, stations have been grouped into regions according to distance from the outfall. The monitoring areas include nearfield stations <2 km from the outfall, nearfield stations > 2 km from the outfall, a transition station, and farfield stations (see Section 2.1).

2.3.1 Data Reduction and Statistics for SPI Images

Details on parameters and analysis of SPI images can be found in Diaz et al. (2008). For this report, quantitative SPI parameters were averaged from the three replicate images. For categorical parameters the median value of the three replicate images was assigned to a station.

Since the selection of station locations in the nearfield was non-random, fixed-effect nominal logistic models were used to analyze patterns in categorical data (Agresti 1990). For continuous variables, general linear models were used to test for differences within and between quantitative parameters. Normality was checked with the Shapiro–Wilk test and homogeneity of variance with Bartlett's test. Trends in quantitative variables were tested using simple linear regression, segmented linear regression, and quasipoisson regression. Significance of odds was tested using logistic regression. All statistical tests were conducted with the statistical package R version 3.5.2 (2018-12-20) "Eggshell Igloo" (The R Foundation for Statistical Computing).

3 RESULTS AND DISCUSSION

3.1 SEDIMENT CONDITIONS

3.1.1 *Clostridium perfringens*, Grain Size, and Total Organic Carbon

Sediment conditions were characterized by three parameters measured during 2018 at each of the 14 sampling stations: (1) *Clostridium perfringens*, (2) grain size (gravel, sand, silt, and clay), and (3) total organic carbon (Table 3-1).

Spores of the anaerobic bacterium *Clostridium perfringens* (reported as colony forming units per gram dry weight, normalized to percent fines) provide a sensitive tracer of effluent solids. A sharp increase *C. perfringens* concentrations at sites within two kilometers from the diffuser occurred coincident with diversion of effluent to the offshore outfall (Figure 3-1). *C. perfringens* concentrations have declined or remained comparable to the baseline at all other monitoring locations during the post-diversion period. *C. perfringens* counts in samples collected during 2018 were lower than the previous year at all nearfield locations, but increased slightly at the transition and farfield sites (Figure 3-1). As in past years during the post-diversion period, *C. perfringens* concentrations during 2018 continued to indicate a footprint of the effluent plume at sites closest to the discharge. Normalized *C. perfringens* spore counts in samples collected in 2018 were highest at station NF17 located within two kilometers of the outfall (Table 3-1, Figure 3-2). The results for *C. perfringens* provide a sensitive "effluent signature", or evidence of low levels of settlement of solids from the effluent at sites in close proximity (within 2 km) to the outfall, as has been seen in previous reporting (e.g. Maciolek et al. 2007, 2008).

Sediment texture in 2018 varied considerably among the 14 stations, ranging from almost entirely sand (e.g., NF17, NF13, and NF04) to predominantly silt and clay (i.e., FF04), with most stations having mixed sediments (Figure 3-3). Sediment texture has remained generally consistent over time, with relatively small year-to-year changes in the percent fine sediments at most stations (Figure 3-4). Annual variability in sediment texture at the Massachusetts Bay stations has typically been associated with strong storms. Sediment transport at water depths less than 50 meters near the outfall site in Massachusetts Bay occurs largely as a result of wave-driven currents during strong northeast storms (Bothner et al. 2002).

Concentrations of TOC in 2018 remained similar to values reported in prior years at most stations (Figure 3-5). Higher TOC values were generally associated with higher percent fines (compare Figures 3-4 and 3-5).

C. perfringens counts continue to provide evidence of low levels of effluent solids depositing near the outfall. There is no indication, however, that the wastewater discharge contributes sufficient solids to result in changes to the sediment grain size composition at the Massachusetts Bay sampling stations, even at stations closest to the outfall. Similarly, there is no indication of organic enrichment. Overall TOC concentrations remain comparable to, or lower than, values reported during the baseline period, even at sites closest to the outfall (Figure 3-6).

Table 3-1. Monitoring results for sediment condition parameters in 2018.

Monitoring Area	Station	*Clostridium perfringens* (cfu/g dry/%fines)	Total Organic Carbon (%)	Gravel (%)	Sand (%)	Silt (%)	Clay (%)	Percent Fines (Silt + Clay)
Transition Area	**FF12**	36.1	0.31	1.9	70.6	22.5	5.1	27.6
Nearfield (<2 km from outfall)	**NF13**	11.4	0.12	0.8	96.4	1.1	1.6	2.7
	NF14	102.0	0.25	33.8	60.6	3.1	2.5	5.6
	NF17	197.8	0.53	0	98.6	0.1	1.3	1.4
	NF24	31.7	0.38	0	72.5	23.3	4.2	27.5
Nearfield (>2 km from outfall)	**NF04**	47.4	0.52	0	98.8	0.1	1.1	1.2
	NF10	24.4	0.44	0	74.0	20.9	5.1	26.0
	NF12	25.8	1.70	0	34.0	49.7	16.3	66.0
	NF20	51.5	0.32	16.4	72.6	9.6	1.4	11.0
	NF21	5.5	0.84	0	46.4	43.6	10.0	53.6
	NF22	33.9	0.98	0	49.3	38.2	12.5	50.7
Farfield	**FF01A**	12.7	0.27	0.4	82.4	14.8	2.5	17.3
	FF04	14.0	2.23	0.2	15.0	58.0	26.8	84.8
	FF09	46.8	0.32	1.9	86.5	6.1	5.4	11.6

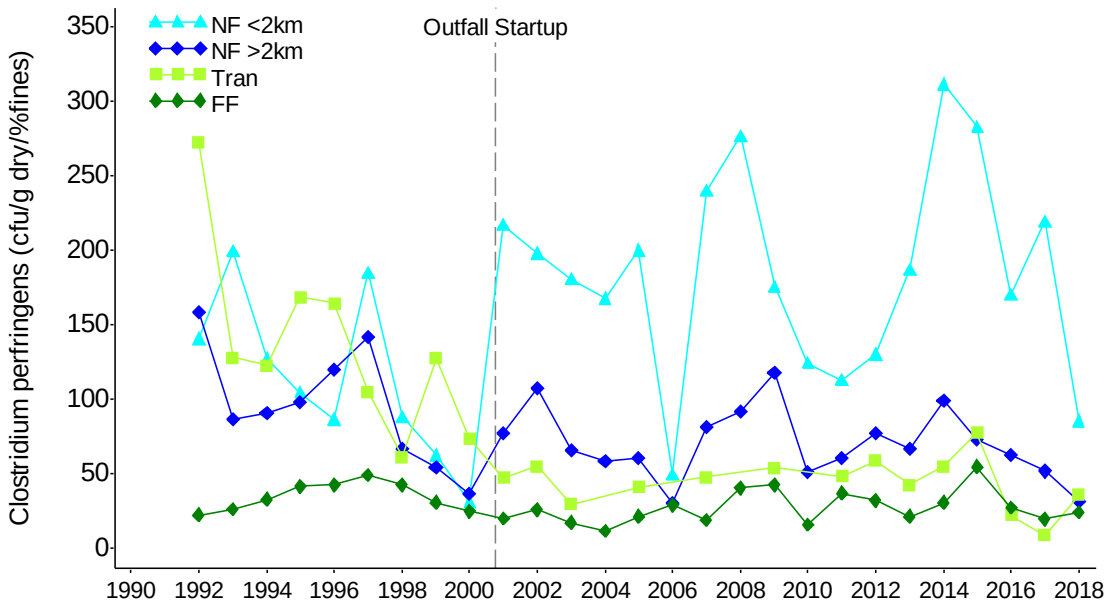

Figure 3-1. Mean concentrations of *Clostridium perfringens* in four areas of Massachusetts Bay, 1992 to 2018. Tran=Transition area; NF<2km=nearfield, less than two kilometers from the outfall; NF>2km=nearfield, more than two kilometers from the outfall; FF=farfield.

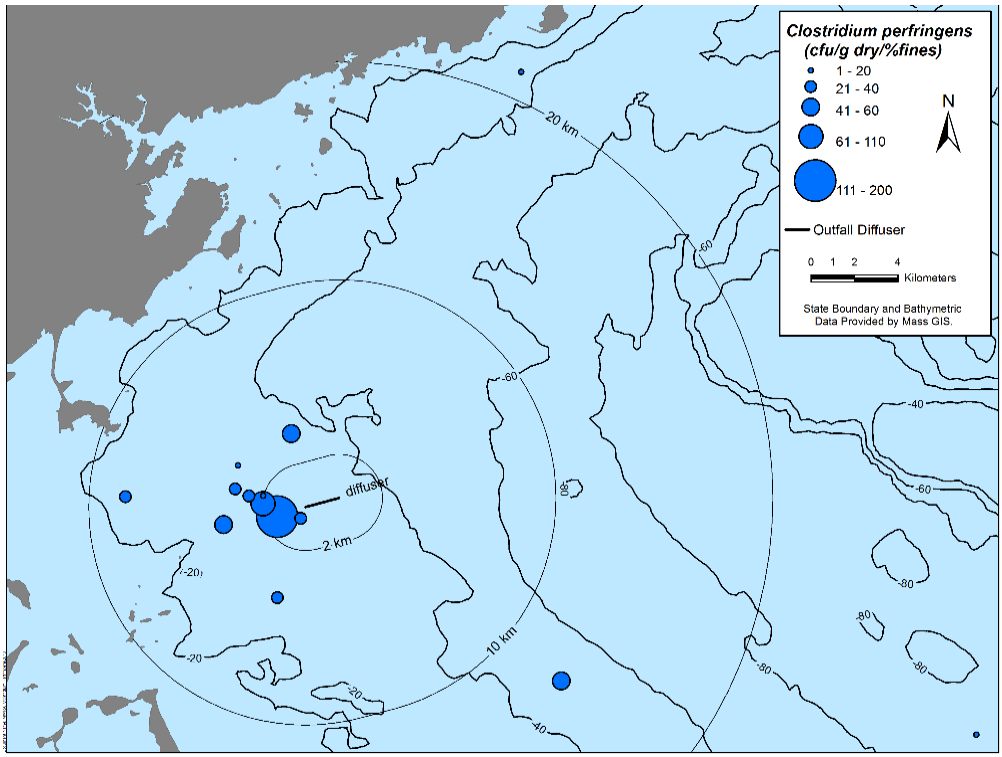

Figure 3-2. Monitoring results for *Clostridium perfringens* in 2018.

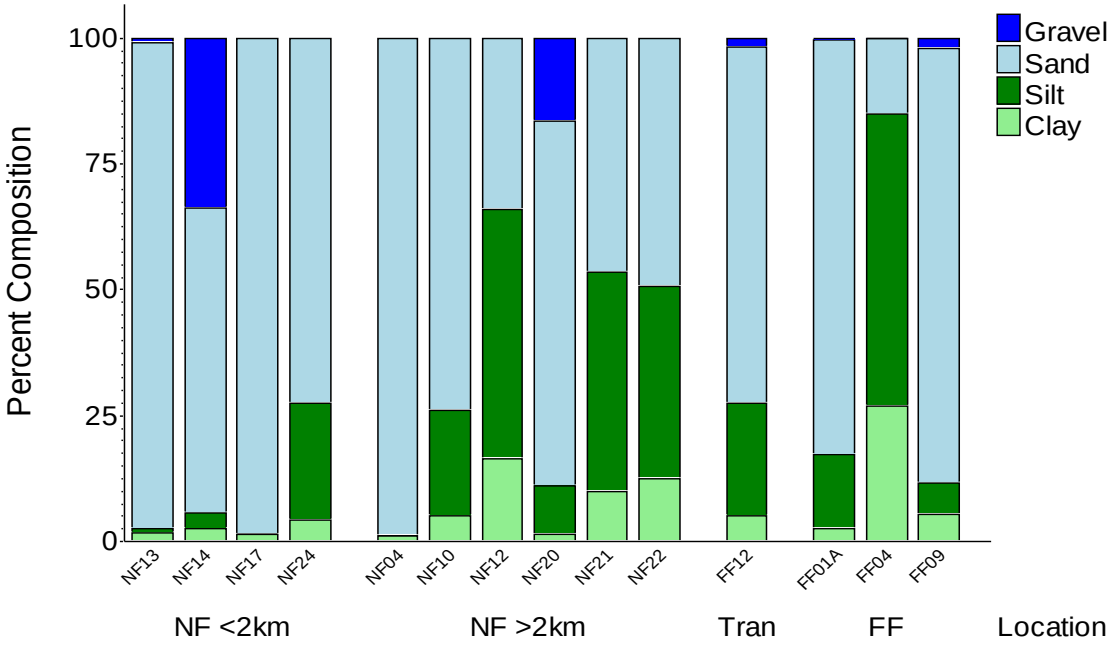

Figure 3-3. Monitoring results for sediment grain size in 2018.

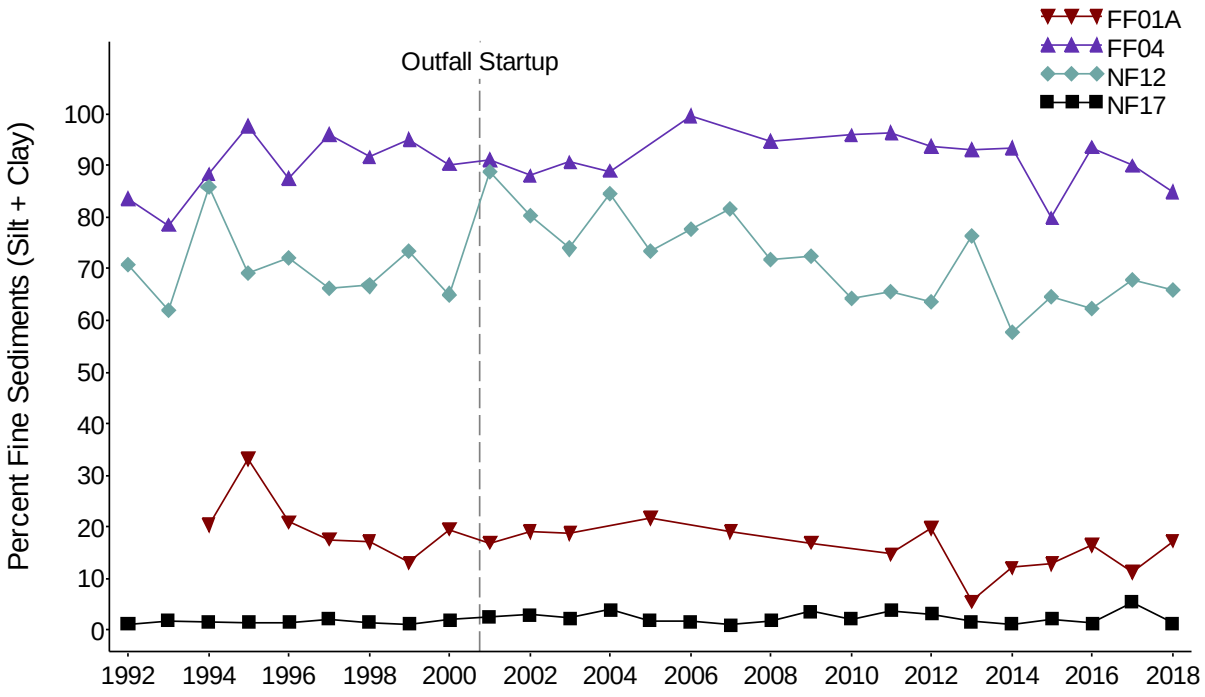

Figure 3-4. Mean percent fine sediments at FF01A, FF04, NF12 and NF17; 1992 to 2018.

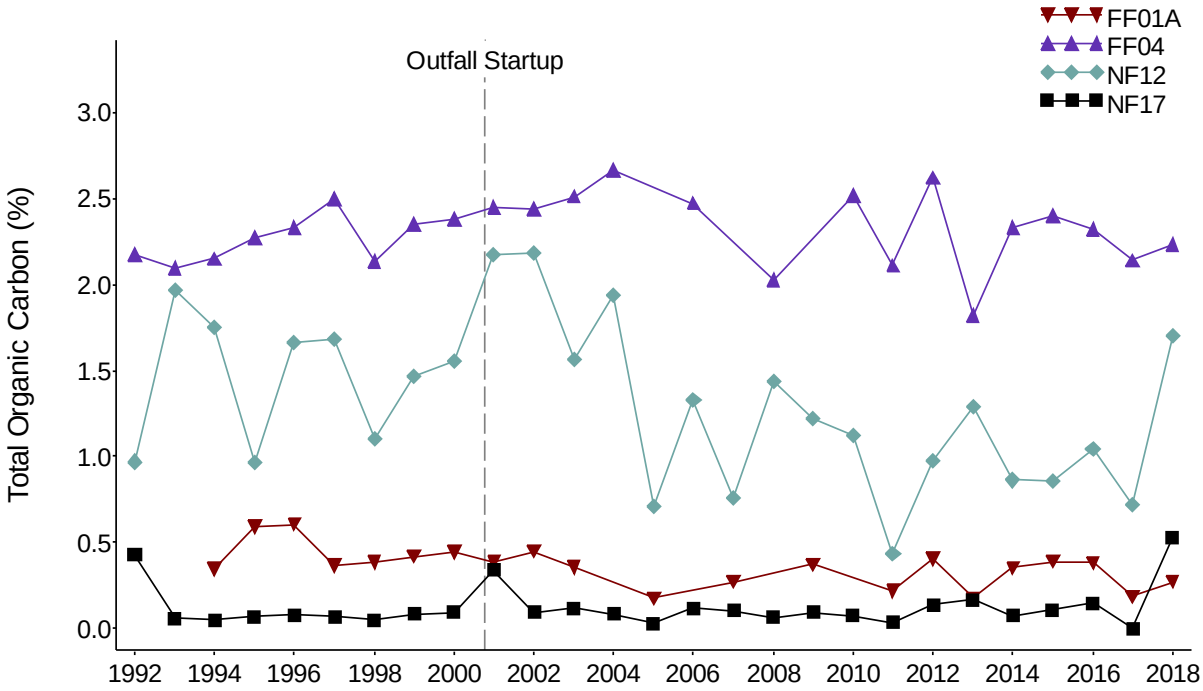

Figure 3-5. Mean concentrations of TOC at four stations in Massachusetts Bay, 1992 to 2018.

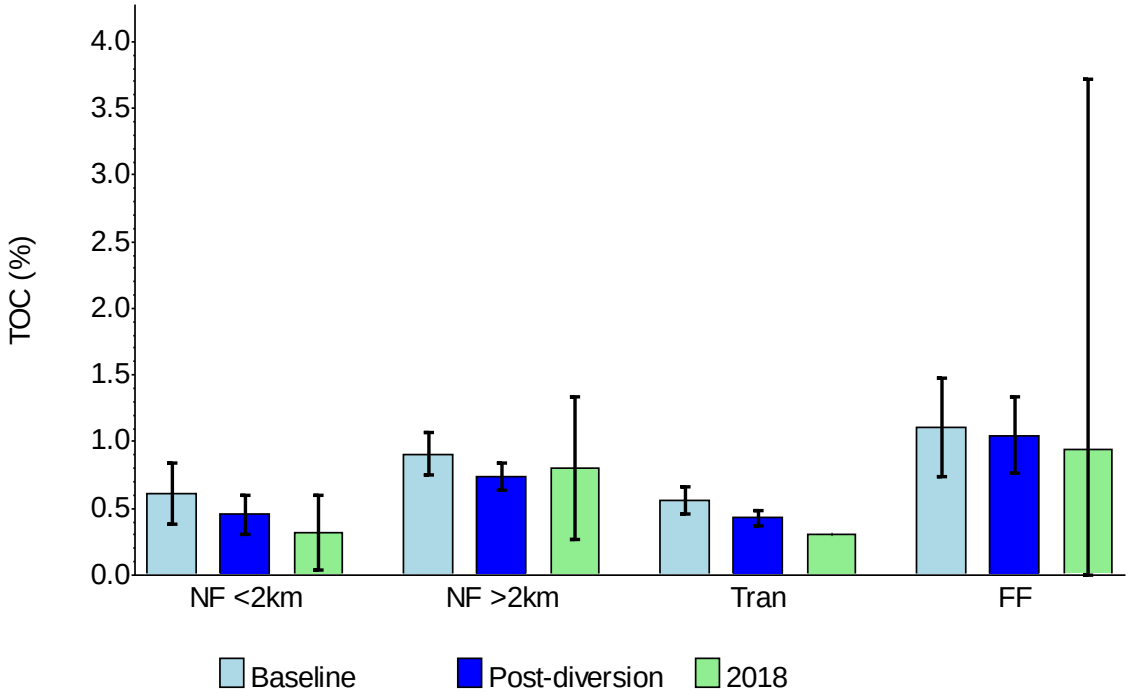

Figure 3-6. Mean (with 95% confidence intervals) concentrations of TOC at four areas in Massachusetts Bay during the baseline (1992-2000) and post-diversion (2001 to 2018) compared to 2018.

3.2 BENTHIC INFAUNA

3.2.1 Community Parameters

A total of 27,352 infaunal organisms were counted from the 14 samples in 2018. Organisms were classified into 195 discrete taxa; 175 of those taxa were species-level identifications. The abundance values reported herein reflect the total counts from both species and higher taxonomic groups, while all diversity measures and multivariate analyses are based on the species-level identifications only (Table 3-2).

Total abundance values in 2018 were higher than the 2017 values at all areas in Massachusetts Bay except the nearfield stations located within 2 kilometers from the discharge (Figure 3-7). Abundance at Station FF12 (the only station in the "Transition Area"), remained higher than means for the other areas in the Bay for a fifth consecutive year (Figure 3-7) although similar abundances were observed at some individual nearfield stations (Table 3-2). The numbers of species per sample in 2018 were lower than in 2017 at all locations except at nearfield stations located further than 2 kilometers from the discharge; as seen since 2014, mean values remained relatively similar across all areas of the Bay (Figure 3-8). There were no Contingency Plan threshold exceedances for any infaunal diversity measures in 2018 (Table 3-3). Upper limit exceedances (compared to baseline period values) had been reported for Shannon-Wiener Diversity (H') and Pielou's Evenness (J') each year from 2010 to 2014. Since then, diversity measures have been within the range in baseline values. In March 2017, the EPA approved MWRA's interim request for modification to the Contingency Plan that removed the upper level thresholds for infaunal diversity parameters because this type of exceedance is not indicative of an outfall effect. Permanent approval for the change was granted in February 2018. In 2018, the values for H' and J were above the low threshold limits (Table 3-3, Figures 3-9 and 3-10).

Spatial and temporal patterns of abundance, species richness, species diversity and evenness generally support the conclusion that there is no evidence of negative impacts caused by operation of the offshore outfall.

Table 3-2. Monitoring results for infaunal community parameters in 2018.

Monitoring Area	Station	Total Abundance (per grab)	Number of Species (per grab)	Log-series alpha	Shannon-Wiener Diversity (H′)	Pielou's Evenness (J')
Transition Area	**FF12**	3763	55	9.13	3.46	0.60
Nearfield (<2 km from outfall)	**NF13**	1150	56	12.37	3.70	0.64
	NF14	1774	71	14.85	4.03	0.65
	NF17	534	52	14.37	4.19	0.73
	NF24	2692	63	11.58	3.65	0.61
Nearfield (>2 km from outfall)	**NF04**	1176	52	11.19	2.49	0.44
	NF10	3227	64	11.32	3.53	0.59
	NF12	2024	60	11.64	3.78	0.64
	NF20	2053	60	11.59	3.71	0.63
	NF21	2748	73	13.79	3.91	0.63
	NF22	2630	63	11.61	3.67	0.61
Farfield	**FF01A**	1397	50	10.16	3.74	0.66
	FF04	902	42	9.14	3.64	0.67
	FF09	1282	78	18.45	4.61	0.73

Table 3-3. Infaunal monitoring threshold results, August 2018 samples.

Parameter	Threshold range		Result	Exceedance?
	Low	High		
Total species	43.0	81.9	60.82	No
Log-series Alpha	9.42	-	12.13	No
Shannon-Weiner H′	3.37	-	3.65	No
Pielou's J'	0.57	-	0.62	No
Apparent RPD	1.18	NA	5.09	No
Percent opportunists	10% (Caution) 25% (Warning)		1.8	No

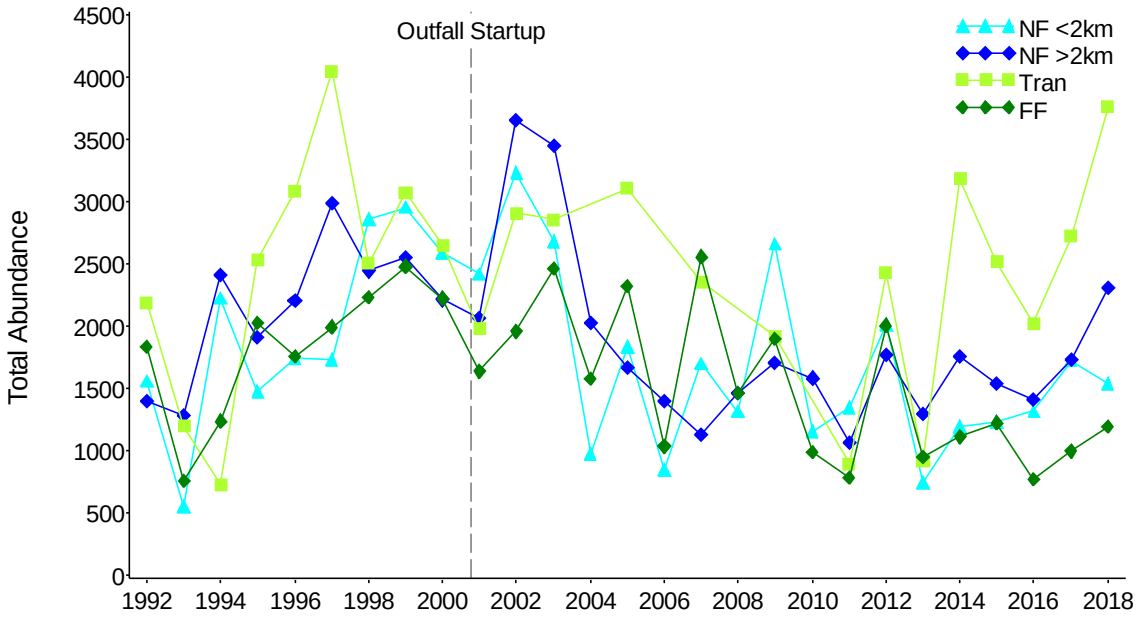

Figure 3-7. Mean infaunal abundance per sample at four areas of Massachusetts Bay, 1992 to 2018. Tran=Transition area; NF<2km=nearfield, less than two kilometers from the outfall; NF>2km=nearfield, more than two kilometers from the outfall; FF=farfield.

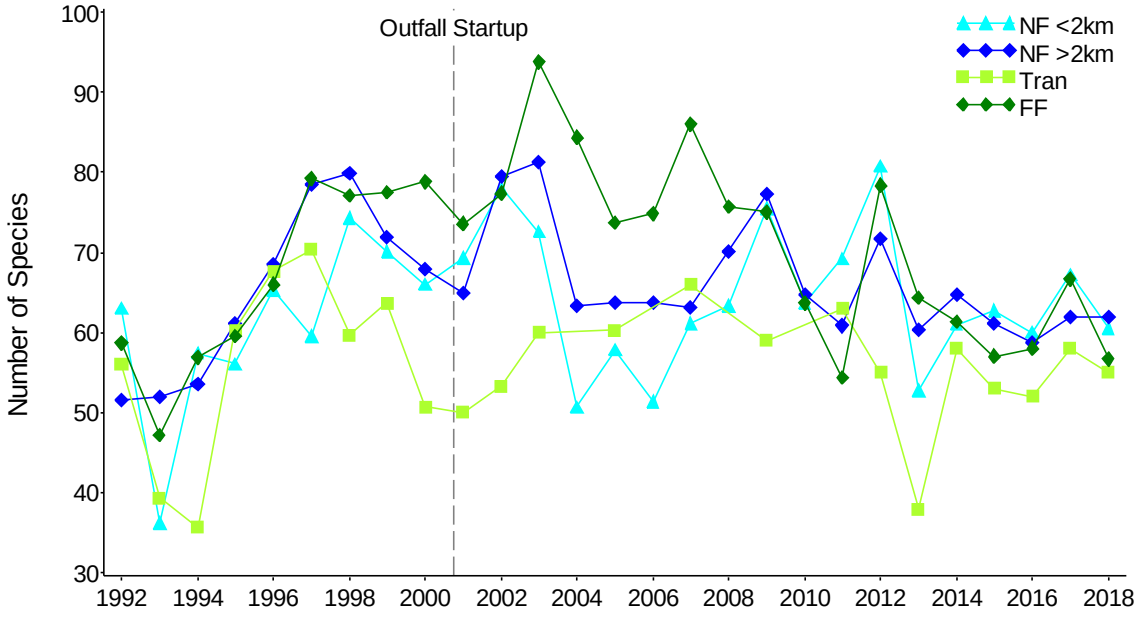

Figure 3-8. Mean number of species per sample at four areas of Massachusetts Bay, 1992 to 2018. Tran=Transition area; NF<2km=nearfield, less than two kilometers from the outfall; NF>2km=nearfield, more than two kilometers from the outfall; FF=farfield.

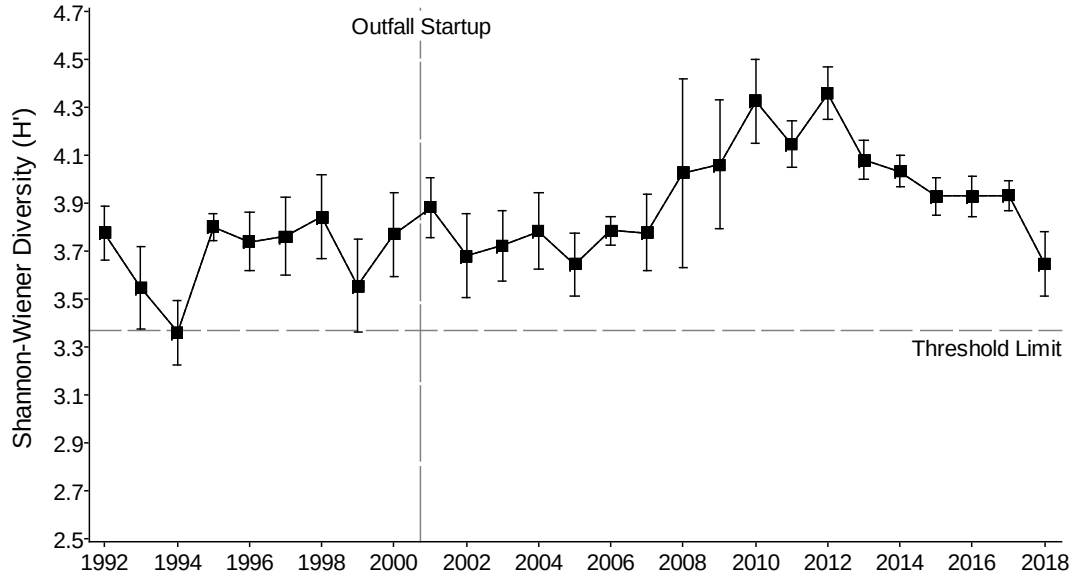

Figure 3-9. Mean (and 95% confidence intervals) Shannon-Wiener Diversity (H′) at nearfield stations in comparison to threshold limit, 1992 to 2018. The nearfield annual means and associated threshold limit are both based on the list of stations sampled following the 2010 revision to the Ambient Monitoring Plan (MWRA 2010).

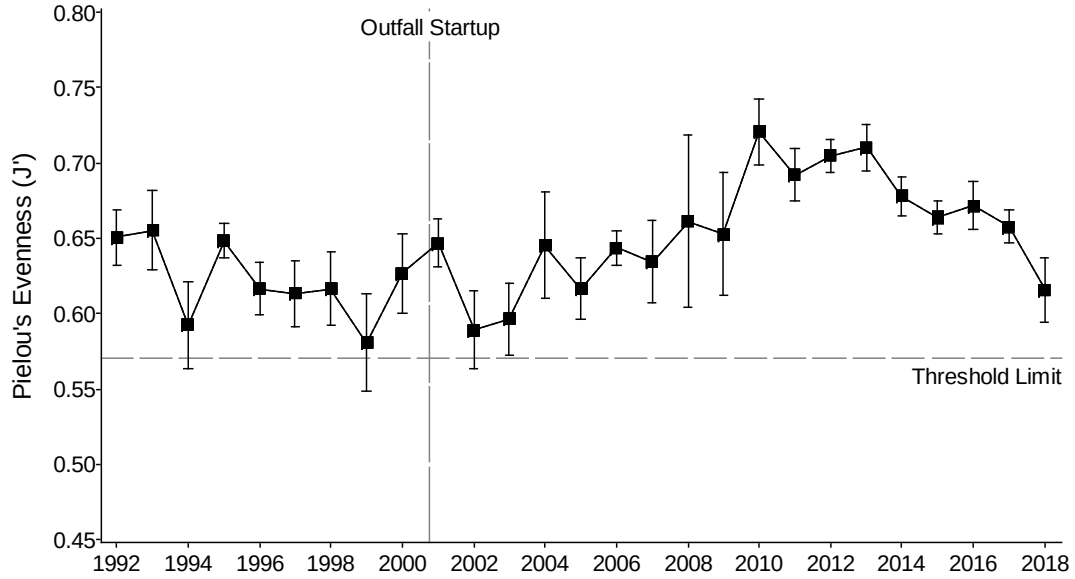

Figure 3-10. Mean (and 95% confidence intervals) Pielou's Evenness (J′) at nearfield stations in comparison to threshold limit, 1992 to 2018. The nearfield annual means and associated threshold limit are both based on the list of stations sampled following the 2010 revision to the Ambient Monitoring Plan (MWRA 2010).

3.2.2 Infaunal Assemblages

Multivariate analyses based on Bray-Curtis Similarity were used to assess spatial patterns in the faunal assemblages at the Massachusetts Bay sampling stations. Two main assemblages (Groups I and II) were identified in a cluster analysis of the 14 samples from 2018 (Figure 3-11). The main groups were distinguished primarily based on the mean abundances and dominant taxa. Abundances at the stations included in Group I were generally two to three times lower than Group II. All assemblages were mostly dominated by polychaetes (Table 3-4). While *Aricidea catherinae* was among the dominants in both groups, three species (*Polygordius jouinae, Crassicorophium crassiorne,* and *Tanaissus psammophilus*) were prevalent only in Group I and four species (*Aricidea quadrilobata, Levinsenia gracilis, Prionospio steenstrupi*, and *Anobothrus gracilis*) were prevalent only in Group II. Group I consisted of no subgroups and was composed of three nearfield stations: NF17, NF04, and NF13. The Group II assemblage included five subgroups (Group IIA: Stations NF12, NF10, NF21, and NF22; Group IIB: Stations NF14, NF24, FF12, and NF20; three single-sample outlier stations: FF09, FF01A, and FF04) that could be differentiated by species composition and total abundance. Species richness at Station FF09 was the highest of any group and Station FF01A was characterized by low species richness (Table 3-2). Similarly, the relatively deep Station FF04 was characterized by low abundances and species richness. Dominant species at Station FF04, including *Levinsenia gracilis, Cossura longocirrata*, and *Chaetozone anasimus*, are characteristic of the soft sediment community observed throughout Stellwagen Basin (e.g., Maciolek et al. 2008).

Both main assemblages occurred at the four stations within two kilometers of the discharge as well as at stations more than two kilometers from the discharge (Figure 3-12). Thus, stations closest to the discharge were not characterized by a unique faunal assemblage reflecting effluent impacts. Comparisons of faunal distribution to habitat conditions indicated that patterns in the distribution of faunal assemblages follow differences in habitat types at the sampling stations and are associated with the sediment types at the sampling stations (Figure 3-13) and with station depth (not shown).

Patterns identified in these analyses were highly consistent with previous years. No evidence of impacts from the offshore outfall on infaunal communities in Massachusetts Bay was found.

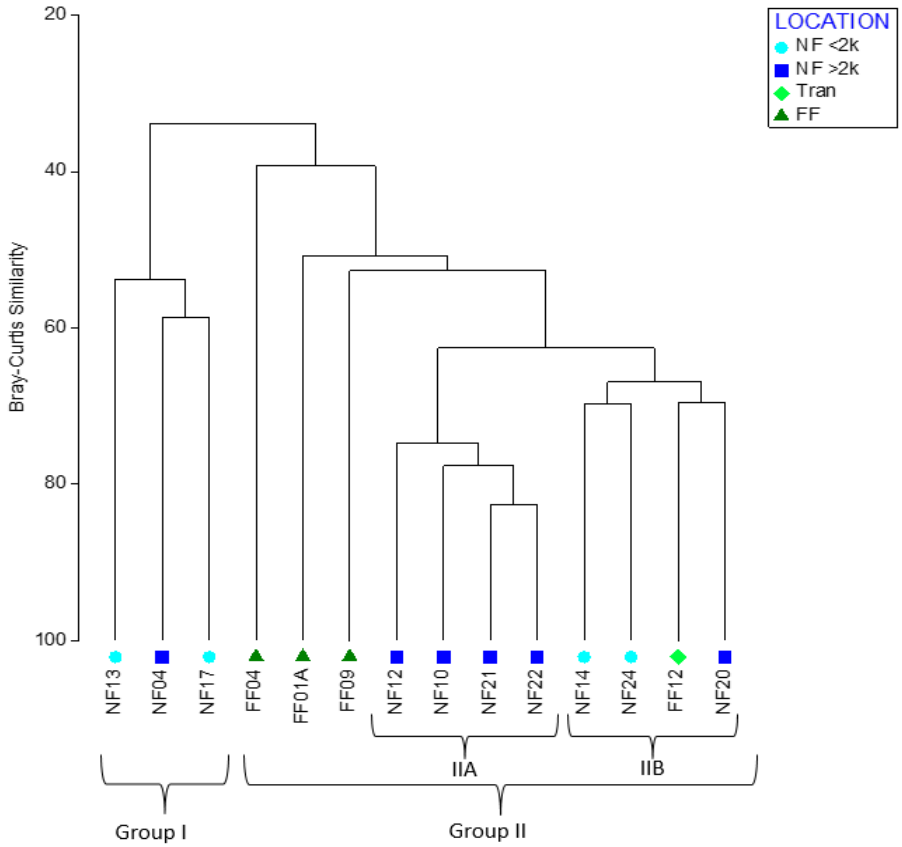

Figure 3-11. Results of cluster analysis of the 2018 infauna samples.

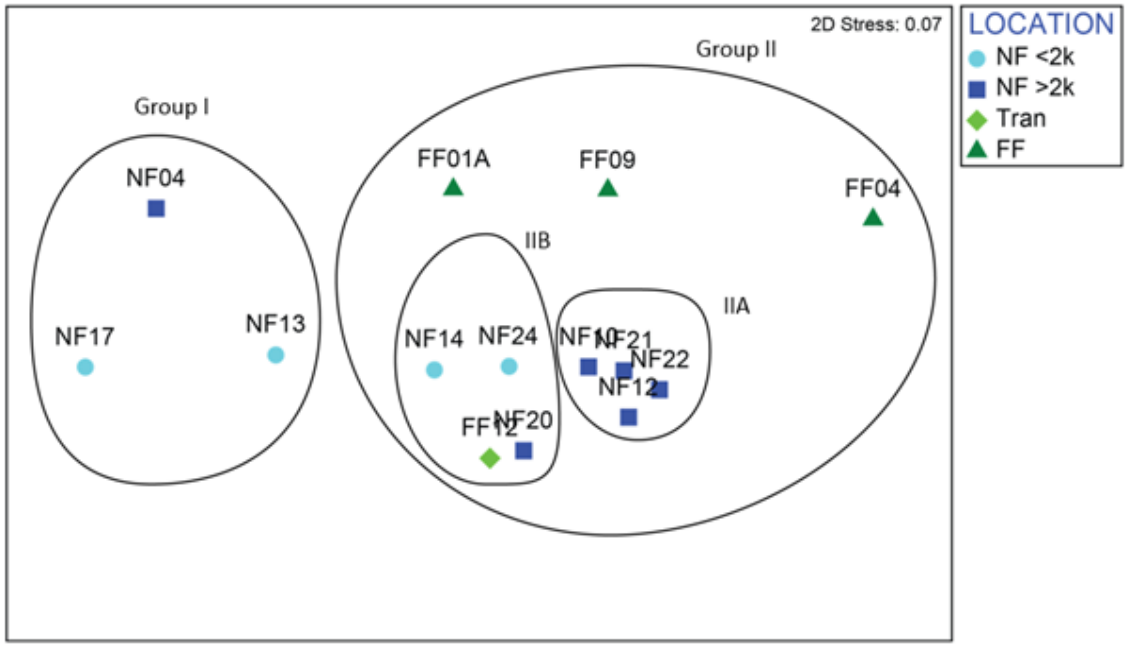

Figure 3-12. Results of a MDS ordination of the 2018 infauna samples from Massachusetts Bay showing distance from the outfall.

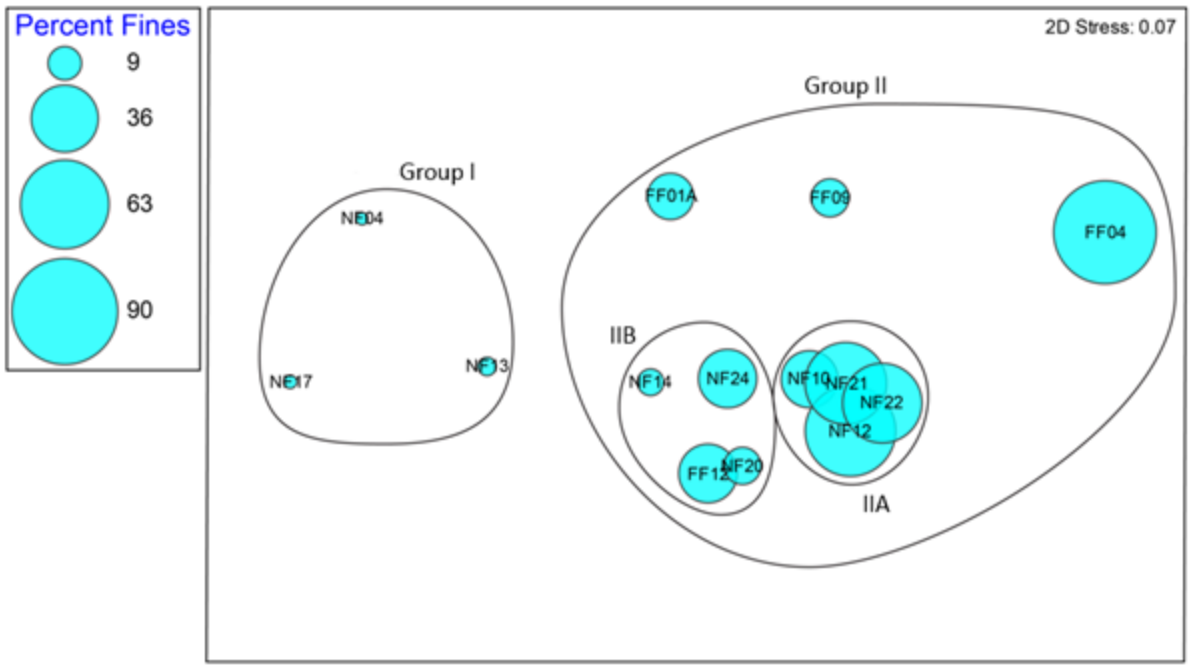

Figure 3-13. Percent fine sediments superimposed on the MDS ordination plot of the 2018 infauna samples. Each point on the plot represents one of the 14 samples; similarity of species composition is indicated by proximity of points on the plot. Faunal assemblages (Groups I-II, and sub-groups) identified by cluster analysis are circled on the plot. The ordination and cluster analysis are both based on Bray-Curtis Similarity.

Table 3-4. Abundance (mean # per grab) of numerically dominant taxa (10 most abundant per group) composing infaunal assemblages identified by cluster analysis of the 2018 samples.

		Group I			Group II				
Family	**Species**	**NF04**	**NF13**	**NF17**	**IIA**	**IIB**	**FF01A**	**FF04**	**FF09**
Nemertea									
	Nemertea sp. 12	-	1	-	7	32.25	-	14	28
Mollusca (Bivalvia)									
Arcticidae	*Arctica islandica*	18	10	1	6.25	3	12	2	3
Mytilidae	*Crenella decussata*	-	2	1	1.75	0.25	-	-	70
Nuculidae	*Ennucula delphinodonta*	2	17	2	26.75	15.5	209	2	231
Periplomatidae	*Periploma papyratium*	-	-	-	8.5	7.75	7	8	53
Pharidae	*Ensis leei*	11	39	3	4	-	-	-	-
Thyasiridae	*Thyasira gouldi*	-	-	-	-	8.5	5	1	43
Annelida (Polychaeta)									
Ampharetidae	*Anobothrus gracilis*	-	-	-	0.75	5.5	1	119	131
Amphinomidae	*Paramphinome jeffreysii*	-	-	-	-	-	-	33	-
Capitellidae	*Mediomastus californiensis*	4	14	1	206.5	363	10	16	46
Cirratulidae	*Chaetozone anasimus*	12	34	5	0.75	-5	-	120	6
	Kirkegaardia baptisteae	-	25	-	155.25	241.25	33	-	-
	Kirkegaardia hampsoni	-	-	-	65.75	75.25	26	-	1
	Tharyx acutus	14	98	1	398	591	58	-	69
Cossuridae	*Cossura longocirrata*	-	-	-	1.25	11.5	-	108	2
Lumbrineridae	*Ninoe nigripes*	-	1	-	60.25	78	35	27	34
Nephtyidae	*Aglaophamus circinata*	27	1	1	0.25	0.25	9	-	1
Orbiniidae	*Leitoscoloplos acutus*	-	-	-	19.25	131.5	7	7	15
Oweniidae	*Owenia artifex*	5	-	6	6..5	4.25	408	-	13
Paraonidae	*Aricidea catherinae*	27	368	12	377.5	611.25	49	-	2
	Aricidea quadrilobata	-	-	-	-	7.5	18	110	88
	Levinsenia gracilis	-	1	-	111.25	214.25	67	199	94
Phyllodocidae	*Phyllodoce mucosa*	8	42	8	83	1.5	5	-	-
Polygordiidae	*Polygordius jouinae*	41	94	120	30.25	7.75	48	-	14
Sabellidae	*Euchone incolor*	-	-	-	4	20	101	46	24
Spionidae	*Polydora cornuta*	-	1	-	168.25	-	1	-	-
	Prionospio steenstrupi	2	2	10	215.75	96.5	145	9	56
	Spio limicola	1	1	-	10	47.5	-	-	7
	Spiophanes bombyx	21	34	1	49.75	9.75	39	-	2
Syllidae	*Exogone hebes*	126	172	27	62.75	12.25	8	-	9
Annelida (Oligochaeta)									
Tubificidae	*Tubificoides apectinatus*	-	23	-	-	-	-	-	-
Arthropoda (Amphipoda)									
Argissidae	*Argissa hamatipes*	1	5	16	4.25	2	2	-	1
Corophiidae	*Crassicorophium crassicorne*	728	16	86	0.75	-	-	-	-
Haustoriidae	*Acanthohaustorius millsi*	-	-	17	-	-	-	-	-
Phoxocephalidae	*Rhepoxynius hudsoni*	9	2	21	-	-	-	-	-
Unciolidae	*Pseudunciola obliquua*	-	-	18	0.25		-	-	-
Arthropoda (Isopoda)									
Chaetiliidae	*Chiridotea tuftsi*	5	1	20	-	-	-	-	-
Arthropoda (Tanaidacea)									

Family	Species	Group I			Group II				
		NF04	NF13	NF17	IIA	IIB	FF01A	FF04	FF09
Nototanaidae	*Tanaissus psammophilus*	13	9	38	0.5		-	-	-
Chordata (Urochordata)									
Molgulidae	*Molgula manhattensis*	1	-	28	0.25	-	-	-	1

3.3 SEDIMENT PROFILE IMAGING

Starting in 1992, Sediment Profile Images (SPI) were collected at a set of unconsolidated sediment stations in the nearfield region around the MWRA ocean outfall (Figure 2-2). The primary objective was to document the impacts of pre- and post-outfall operation on benthic habitat of infaunal communities and to measure the depth of the apparent color redox potential discontinuity (aRPD) layer as described in the MWRA's Contingency Plan (MWRA 2001). Over the past 27 years most of the changes in habitat conditions occurred over the entire nearfield and were not related to outfall operation (Nestler et al. 2018). This lack of outfall impacts is typical of outfalls located in high energy regions such as the nearfield area where tidal or storms induced currents are the main sources of bottom energy (Signell et al. 2000, Warner et al. 2008, Puente and Diaz 2015). Clover Point, British Colombia, Canada, is an example of a tidally dominated outfall (Chapman et al. 1996) and Mar del Plata City, Argentina, an example of storm dominated outfall (Elías et al. 2005). At both outfalls strong tidal and storm currents lessen outfall impacts on the benthos.

The principal factors effecting benthic habitats across the nearfield appeared to be storms and storm-driven sediment transport (Butman et al. 2008, Warner et al. 2008). Bottom stress associated with storms in Massachusetts Bay and elsewhere is a dominant cause of resuspension of bottom sediments (Butman et al. 2008). In the report on 2017 outfall benthic monitoring results, the Butman et al. (2008) timeline of major storms between 1990 and 2006 was compared to benthic monitoring results for the 1992-2006 periods in which there was overlap. This comparison revealed evidence supporting the hypothesis that storm driven sediment transport impacted nearfield sediments and infaunal communities (Nestler et al. 2018). To further assess how storm related factors effected benthic habitat, sediments, and benthic communities, we calculated integrated wind and wave stress for all storms from January 1990 (20 months prior to the start of nearfield monitoring) to January 2019. We then conducted an exploratory data analysis to further investigate these possible impacts.

Our definition of a storm was based on Butman et al. (2008) who used both wind stress and bottom-wave stress at water depths of 30 m. A storm based on wind stress was defined as a period when winds exceeded 22 knots, producing a stress of 0.2 Pa, for at least 6 h. Integrated wind stress (IWindS) is the sum of the magnitudes of the hourly wind stress for the duration of the storm. Its units are Pascal hours (Pa h). Based on bottom-wave stress a storm was defined as a period when the bottom stress caused by waves was greater than 0.1 Pa for at least 6 h. A bottom stress of 0.1 Pa was used as the threshold to define a storm on the sea floor as it is the stress required to initiate motion of very-fine-sand (4 Phi) and is taken as an approximate threshold for resuspension of fine-grained sediments typical of Massachusetts Bay (Butman et al. 2008). Integrated excess bottom stress caused by waves (IWaveS) was defined as the sum of the magnitude of the bottom stress for a depth of 30 m (the approximate depth of nearfield stations), minus the threshold of 0.1 Pa, for the duration of the storm. Units of IWaveS are also Pascal hours (Pa h). Storm parameters were summarized for the winter year or period prior to the August monitoring (the 8-months from October through May, Butman et al. 2008). For example, storm data related to August 1992 monitoring data would be October 1991 to May 1992.

Storms

From January 1990 to January 2019 there were a total of 832 IWindS and 575 IWaveS storms. The year 2012 was not included as data were not available for 72% of the year. For other years, there were at most 25% missing data between October and May. Most storms (88%) occurred during the winter period (October through May), as did the strongest storms. Storms from June through September were smaller and had lower energy (Figure 3-14).

For winter periods 1991 to 2018, integrated wind stress increased (linear regression of year with October-May sum of IWindS, Slope = 3.857 Pa h/year, $R^2 = 0.28$, df = 25, p = 0.005; Figure 3-15). There was a trend for a long-term increase in winter period integrated bottom stress caused by waves (IWaveS) similar to that of IWindS, though the p value was not significant (Slope = 3.857 Pa h/year, $R^2 = 0.09$, df = 25, p = 0.129). The total number of winter period IWindS and IWaveS storms also trended upward by about 1.4 storms per decade between 1991 and 2018 (total IWindS storms, Slope = 0.138 storm/year, $R^2 = 0.08$, df = 25, p = 0.145 and total IWaveS storms, Slope = 0.076 storm/year, $R^2 = 0.05$, df = 25, p = 0.269; Figure 3-15).

The total duration of IWindS storms increased by about 9 hours per year (linear regression of year with sum of IWindS duration in hours, Slope = 8.738 h/year, $R^2 = 0.24$, df = 25, p = 0.009). The mean duration per IWindS storm tended to be longer but was not significant ($R^2 = 0.11$, df = 25, p = 0.096). Total ($R^2 = 0.06$, df = 25, p = 0.203) and mean duration ($R^2 = 0.07$, df = 25, p = 0.175) for IWaveS storms also tended to increased but not significantly (Figure 3-16).

Factors that go into generation of IWindS and IWaveS storms are complex and act at broad regional scales. For example, duration of storms defined by IWaveS tend to be longer than storms defined by IWindS due to waves generated in the Gulf of Maine that propagate into Massachusetts Bay as the storm systems travel northeastward and after local winds have decreased (Butman et al. 2008). Wind direction is also important component with north and east winds producing the largest storms in the nearfield regions. From 1990 to 2018, about 30% of IWindS storms had winds from the north, northeast, or east (Figure 3-17).

The number of IWindS and IWaveS storms were correlated (r = 0.42, t = 2.2602, df = 24, p = 0.033). The correlation is to be expected: waves are driven by winds. Many IWindS storms were not identified as IWaveS storms, because waves respond to wind direction and non-local winds, but IWindS is based solely on local wind speeds.

The five stormiest years since 1991, based on integrated stress summed for both IWindS and IWaveS, occurred from 2005 to 2018. They were 2013, 2010, 2018, 2005, and 2015, respectively (Figure 3-18). The year 2013 was the stormiest year for both IWindS and IWaveS. Major storms, defined as being in the top 50 from 1991 to 2018 occurred within 6-months of the August monitoring during these years. Least stormy years were 2002 and 1999 followed by 1995, 1991, and 2014. In 1999, 2002 and 2014 at least 18-months passed without a major storm prior to August monitoring. In 1995, a major storm occurred 6-months before August (Figure 3-18).

These analyses of wind and wave stress observed between 1991 and 2018 confirm the evaluations made in the 2017 outfall benthic report (Nestler et al. 2018), that storm events significant enough to impact bottom sediments in Massachusetts Bay are common events. Further, there is substantial evidence that storm impacts on nearfield sediments may have increased over this same period.

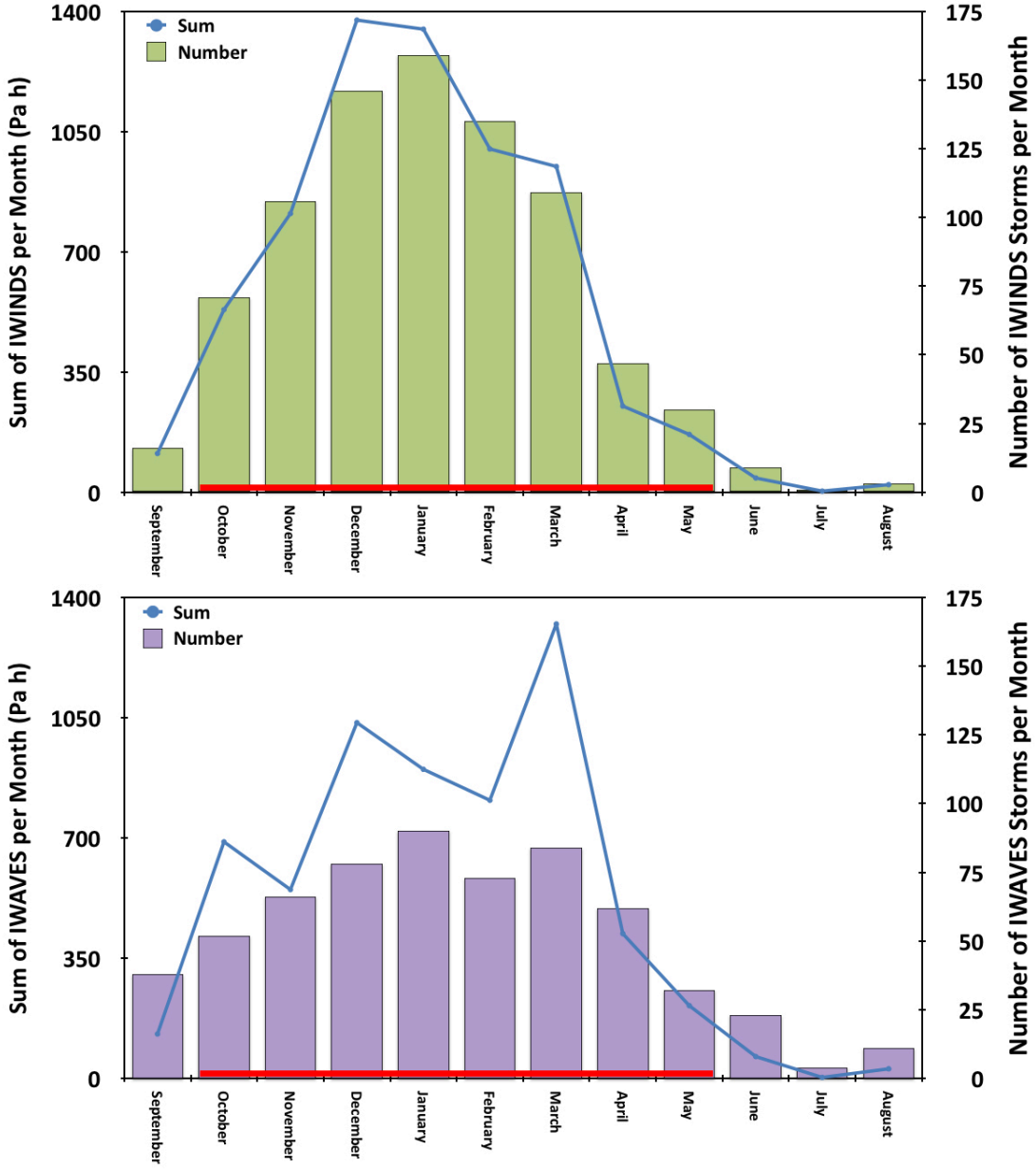

Figure 3-14. Monthly summary of IWindS and IWaveS storms from 1991 to 2018. Storm parameters were summarized by winter period (red line) for analysis.

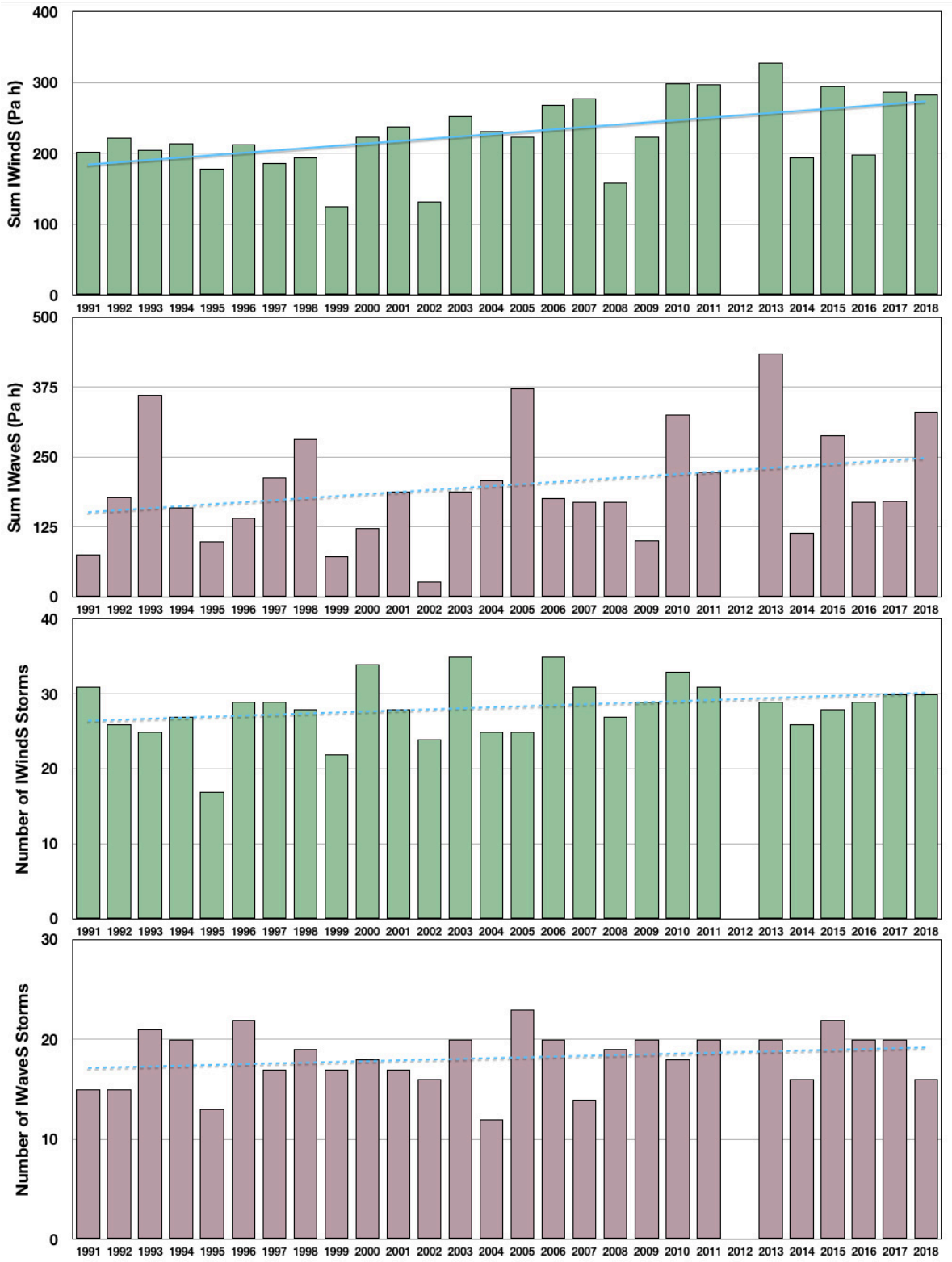

Figure 3-15. Sum and number of IWindS and IWaveS storms for the winter period (October through May) prior to August monitoring. Solid line is a significant increase and dotted lines are nonsignificant trends. The year 2012 was not included due to missing data.

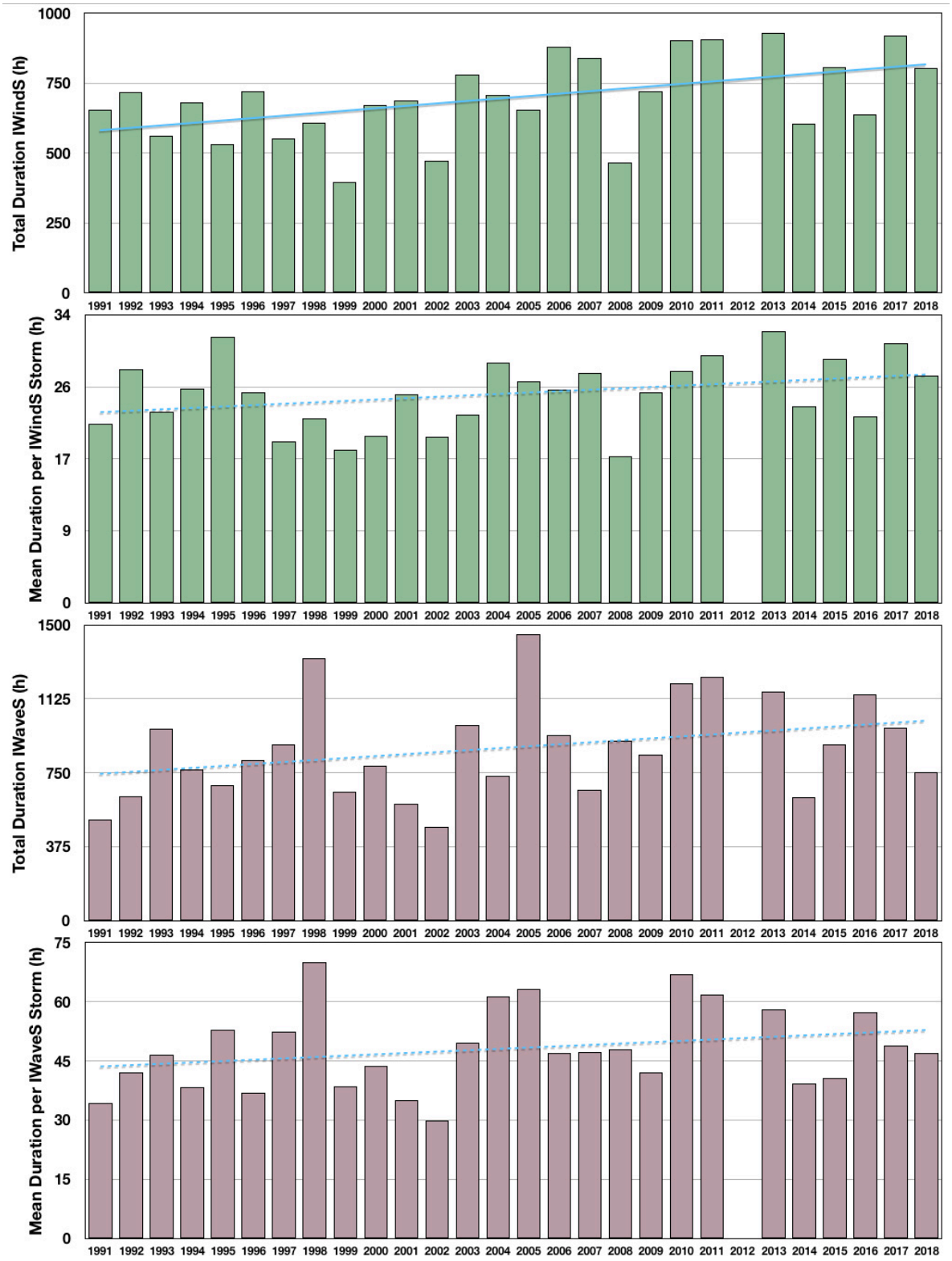

Figure 3-16. Total duration and mean event duration of IWindS and IWaveS for the winter period (October through May) prior to August monitoring. Solid line is a significant increase and dotted lines are nonsignificant trends. The year 2012 was not included due to missing data.

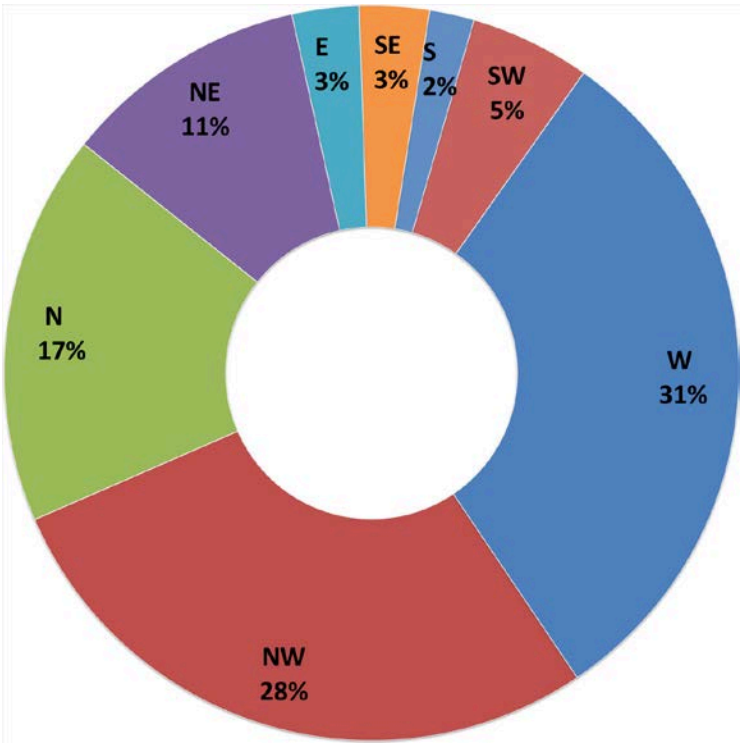

Figure 3-17. Summary of wind direction for winter period (October through May) IWindS storms from 1991 to 2018.

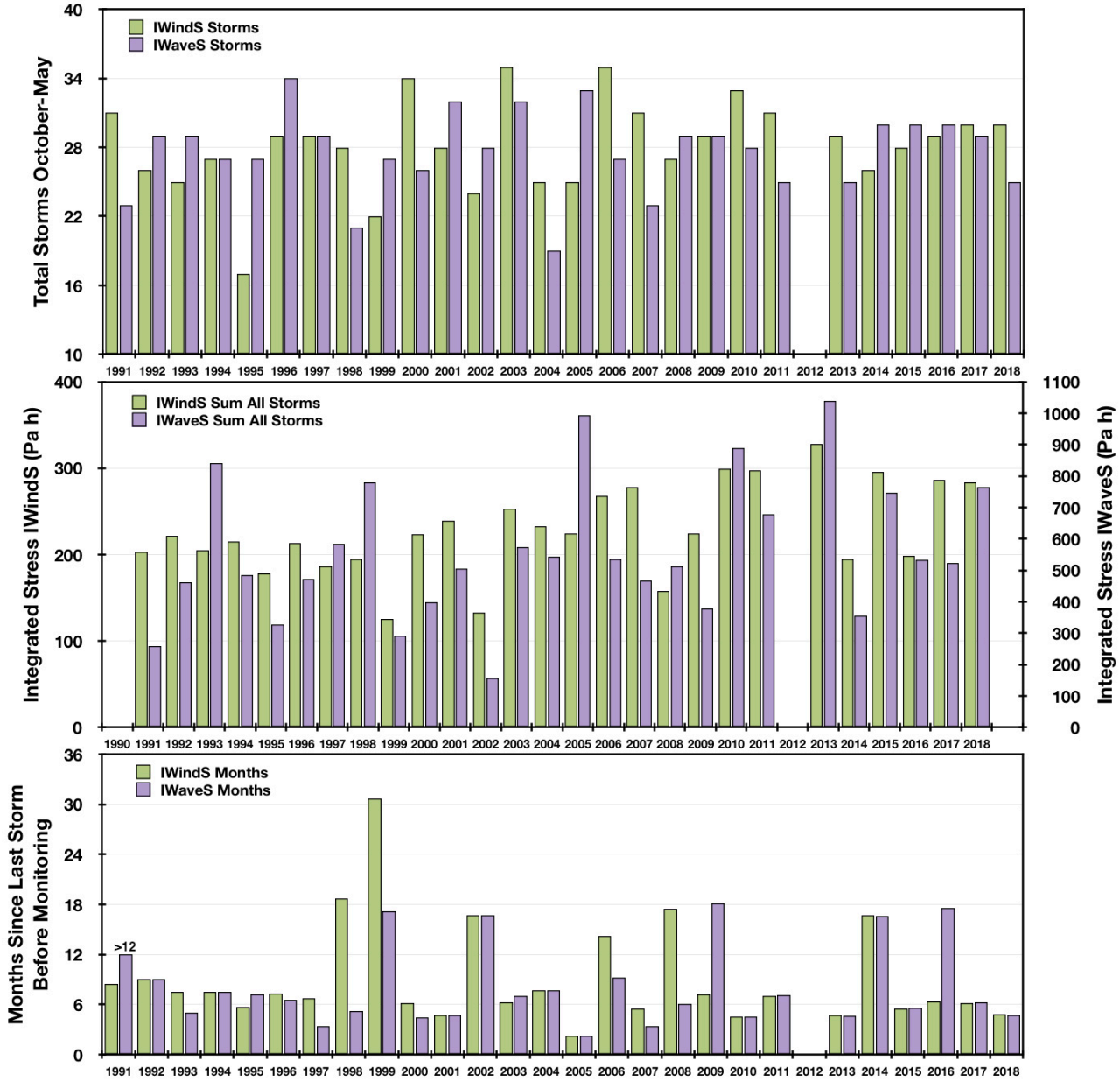

Figure 3-18. Winter period (October through May) storm frequency, strength, and length of time since last major storm before August from 1991 to 2018. The year 2012 was not included due to missing data.

Sediments

Sediments at the nearfield stations ranged from fine-sand-silt-clay to cobble with most stations having uniform estimated modal grain-size and percent fines (silt + clay) though time (NF12 for example, Figures 3-4 and 3-19). Sediments at some stations were more temporally heterogeneous (NF02 for example, Figure 3-20). Storms could affect sediment grain-size through resuspension events that exceed the critical erosion threshold, which represents stability/erodability of the bed (Thompson et al. 2017). The threshold for defining IWaveS storms was a critical stress of 0.1 Pa, which would resuspend very-

fine-sand (4 Phi) and finer sediments. Fine-sand (3 Phi) would be resuspended by 0.14 Pa (Butman et al. 2008).

Variation in estimated modal grain-size from SPI through time was not significantly related to the intensity of winter period storms at most stations (Table 3-5). For annual sum of IWaveS, there was a significant negative relationship with modal grain-size (suggesting that sediments coarsened) at two stations (NF24 and NF15) and a marginally significant relationship at a third station (NF05). Similarly, there were a few significant negative relationships between the total number of storms and modal grain-size (Stations FF10, NF04, and NF17), with four stations marginally significant (FF13, NF05, NF07, and Nf15). The number of major storm-free months prior to August and grain size were not related, except for Station NF18 (Table 3-5). At Station NF18, there was a positive relationship between storm-free months and grain-size indicating finer sediments were associated with longer times since the last storm. Overall, the total number of storms was most strongly related to modal grain-size, indicating repeated resuspension/deposition events could be more important than single large storm events (Figure 3-21).

In contrast to modal grain-size, median grain-size (estimated graphically using cumulative percentage weights of Phi intervals from sediment analysis at the 11 stations sampled at least 18 time from 1995 to 2018) coarsened as the total number of winter period IWaveS storms increased at 8 of the 11 stations, and was marginally significant at one additional station (NF14, Table 3-6, Figure 3-22). For annual sum of IWaveS, only Station NF14 had a significant negative slope with Station NF13 being marginally significant indicating that median grain-size tended to coarsened with increasing IWaveS. There was no relationship between median grain-size and the number of major storm-free months prior to August monitoring. The significant negative relationships between total number of storms and median grain-size also indicated repeated resuspension/deposition events could be more important than single large storm events leads to a coarsening of grain size at the sampling stations.

Between 2014, a low storm year, and 2015, a high storm year, modal grain-size at five stations (FF12, NF02, NF07, NF10, and NF17) became coarser, likely in response to increased winter period storms in 2015 (Figure 3-23). The shift in modal grain-size at Station NF17 was the most pronounced of all stations, going from fine-medium-sand in 2014 to medium-sand in 2015 and 2016, and back to fine-medium-sand in 2017 and 2018 (Figure 3-23). There were fewer storms in 2014 relative to 2015. In 2014, the last major storm occurred about 17 months prior to August and in 2015 it was about 6 months prior to August (Figure 3-18).

This pattern of SPI modal grain-size coarsening was not observed for the other four stormiest years (2005, 2010, 2013, and 2018), when there were just as many stations that became finer as became coarser. The patterns for median and modal Phi grain-size were similar to SPI estimated modal grain-size. In addition to storm effects, part of the variation in grain-size was due to small-scale within station spatial heterogeneity. For example, change in sediments at NF02 for 2018 appeared to be related to within-station heterogeneity (Figures 3-20 and 3-23).

Table 3-5. Slopes from linear regression and p-value of modal grain-size (Phi) with winter period IWaveS summed from October to May, total number of storms for this period, and the months since the last major storm prior to August monitoring.

	IWaveS Sum		Total Number Storms		Months Since Last Storm	
Station	**Slope**	**p**	**Slope**	**p**	**Slope**	**p**
FF10	0.001	0.861	-0.397	0.031	-0.103	0.207
FF12	-0.001	0.464	-0.060	0.140	0.012	0.492
FF13	-0.002	0.565	-0.256	0.099	0.031	0.639
NF02	-0.002	0.688	-0.156	0.332	-0.009	0.906
NF04	-0.001	0.314	-0.060	0.029	0.007	0.599
NF05	-0.004	0.093	-0.128	0.081	0.022	0.534
NF07	-0.001	0.608	-0.139	0.073	0.018	0.622
NF08	0.000	0.889	0.022	0.588	0.000	0.980
NF09	-0.002	0.268	-0.060	0.381	0.014	0.654
NF10	-0.002	0.372	-0.104	0.167	0.034	0.337
NF12	0.001	0.542	0.027	0.357	-0.005	0.710
NF13	0.000	0.701	-0.025	0.572	-0.013	0.501
NF14	-0.002	0.278	-0.036	0.648	0.054	0.132
NF15	-0.005	0.034	-0.134	0.095	0.037	0.328
NF16	0.000	0.949	-0.107	0.336	0.016	0.763
NF17	0.000	0.706	-0.040	0.024	-0.002	0.809
NF18	-0.002	0.176	0.020	0.748	0.052	0.054
NF19	-0.001	0.753	-0.089	0.335	0.059	0.149
NF20	0.000	0.874	0.087	0.248	0.041	0.232
NF21	0.000	0.529	0.034	0.209	-0.002	0.859
NF22	0.000	0.734	-0.008	0.737	-0.003	0.758
NF23	-0.001	0.564	-0.017	0.778	0.027	0.323
NF24	-0.004	0.010	-0.032	0.575	0.024	0.348

Table 3-6. Slopes from linear regression and p-value of median grain-size (Phi) estimated from the subset of stations sampled at least 18 times from 1995 to 2018 with winter period IWaveS summed from October to May, total number of storms for this period, and the months since the last major storm prior to August monitoring.

	IWaveS Sum		Total Number Storms		Months Since Last Storm	
Station	**Slope**	**p**	**Slope**	**p**	**Slope**	**p**
FF12	0.000	0.834	-0.109	0.029	0.002	0.928
NF04	-0.001	0.195	-0.079	0.007	0.008	0.517
NF10	-0.001	0.372	-0.122	0.009	0.010	0.633
NF12	0.000	0.610	-0.018	0.038	-0.002	0.711
NF13	-0.002	0.059	-0.086	0.003	0.010	0.455
NF14	-0.005	0.038	-0.145	0.098	0.041	0.248
NF17	0.000	0.548	-0.049	0.030	-0.006	0.587
NF20	-0.002	0.396	-0.157	0.045	-0.014	0.676
NF21	-0.001	0.281	-0.050	0.016	0.005	0.586
NF22	0.001	0.410	-0.080	0.126	-0.015	0.496
NF24	0.000	0.842	-0.081	0.318	0.005	0.882

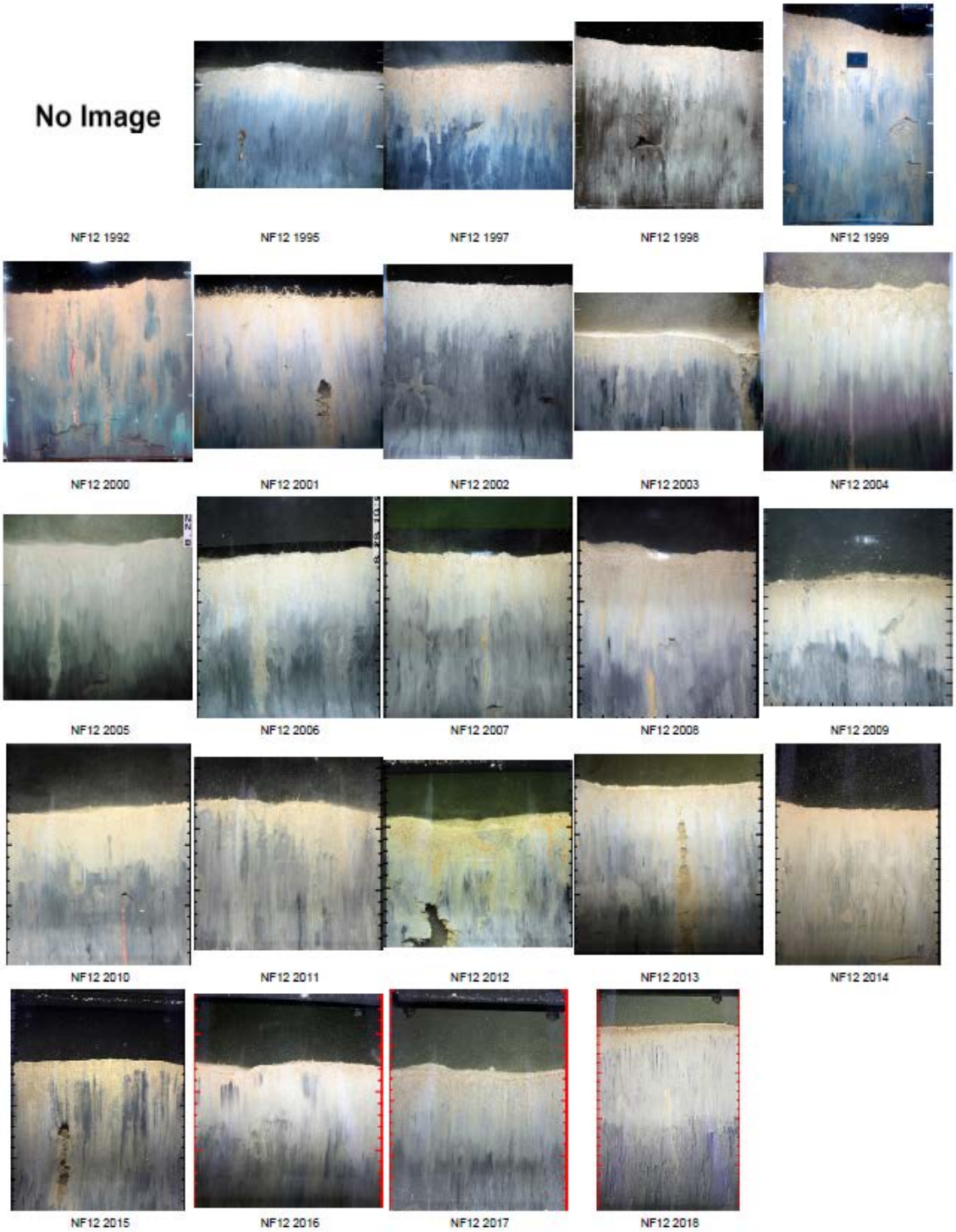

Figure 3-19. Mosaic of images from Station NF12 with homogeneous sediments through time. Scale on side of images is in cm.

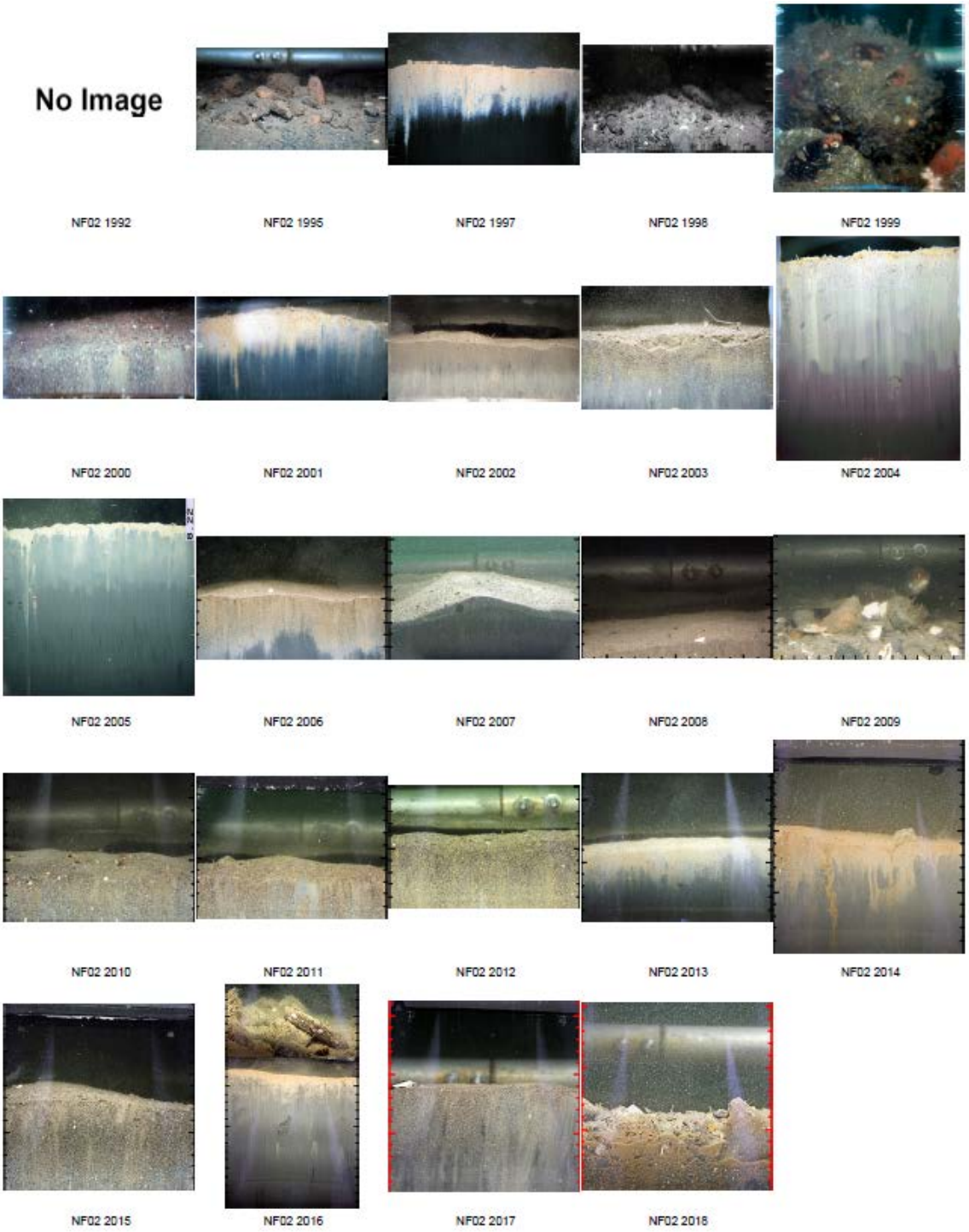

Figure 3-20. Mosaic of images from Station NF02 with heterogeneous sediments through time. Scale on side of images is in cm.

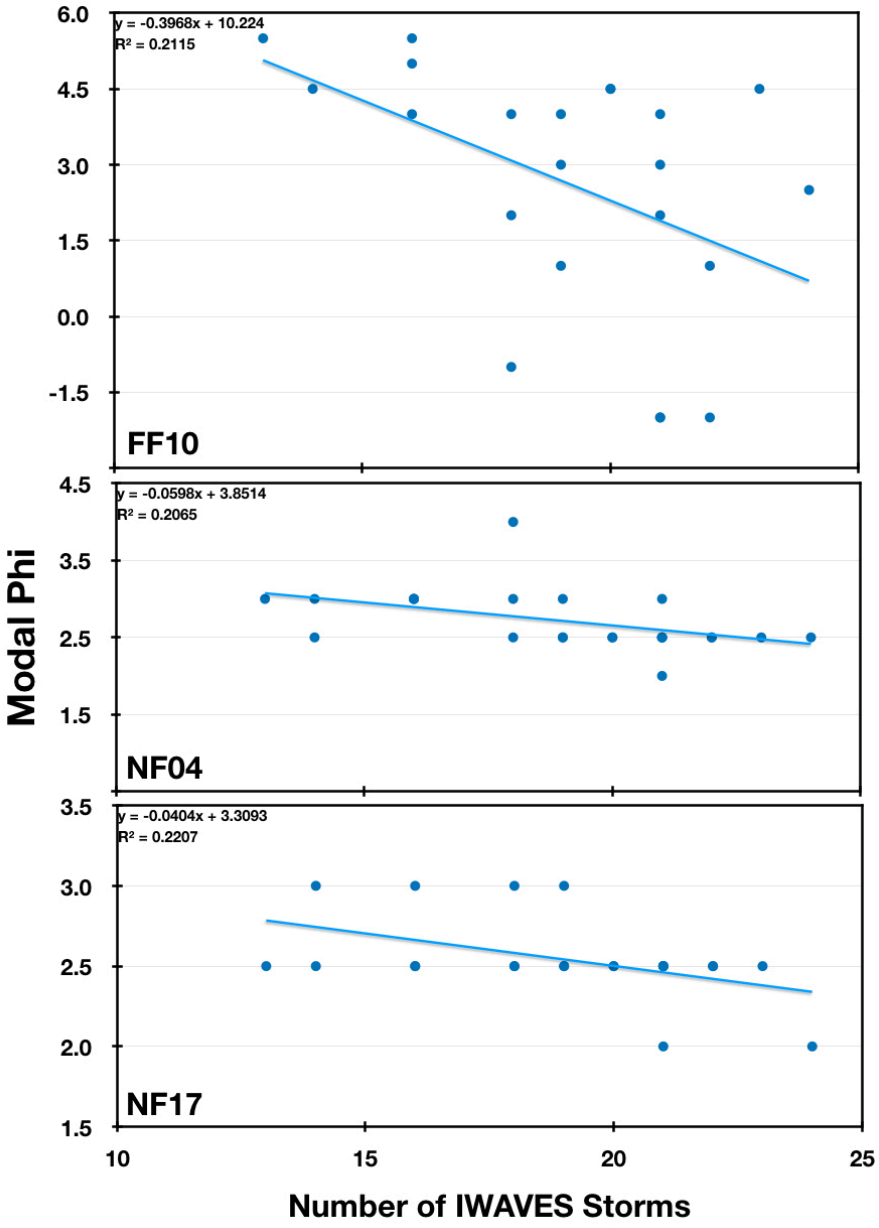

Figure 3-21. Relationship of modal grain-size (Phi) from SPI to number of winter period IWaveS storms at Stations FF10, NF04, and NF17. As modal Phi decreased, sediments became coarser-grained.

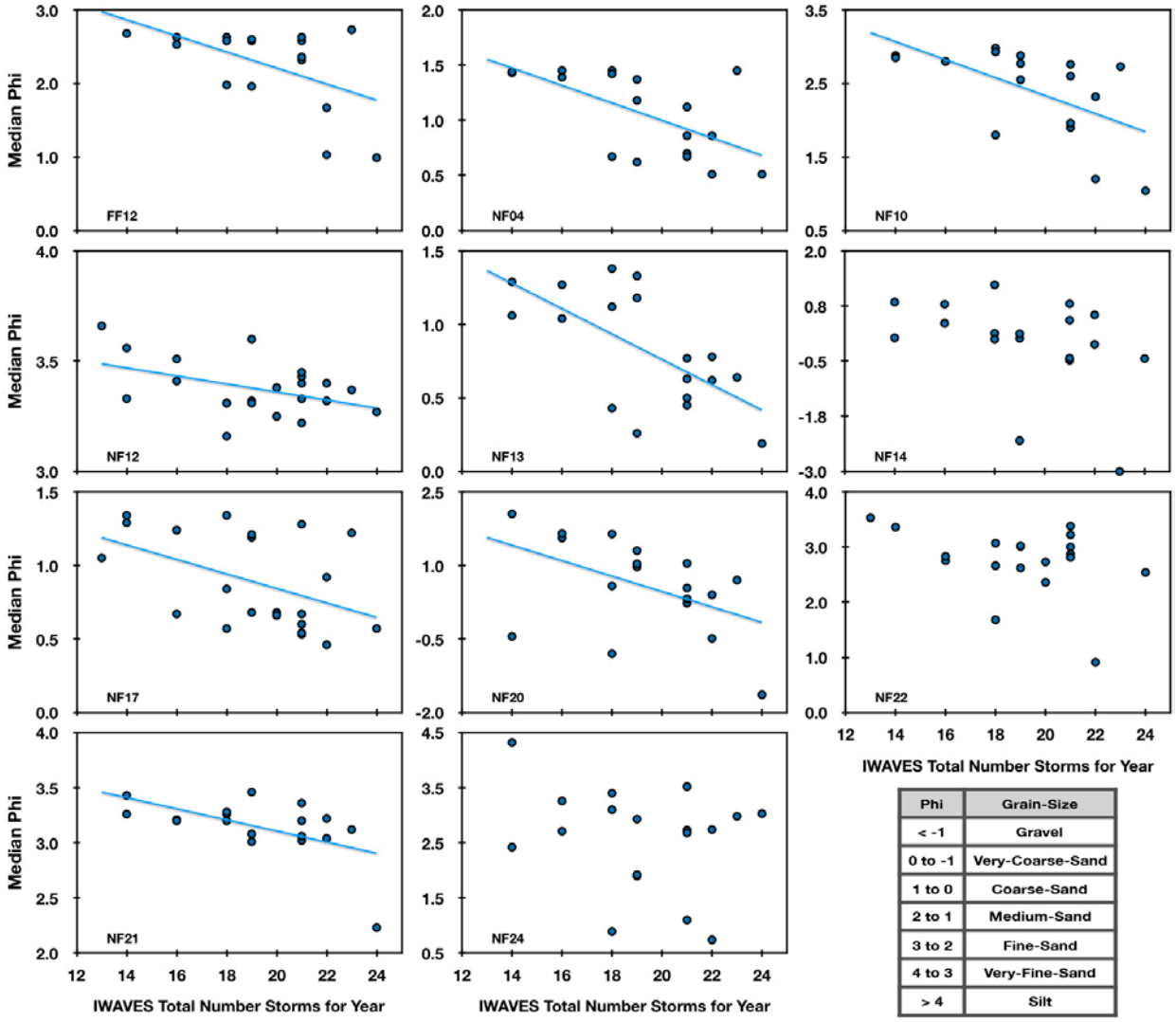

Figure 3-22. Relationship of median grain-size (Phi) from sediment analysis of the subset of stations sampled at least 18 times from 1995 to 2018 to number of winter period IWaveS storms. Station plots with regression lines are significant at p = <0.05.

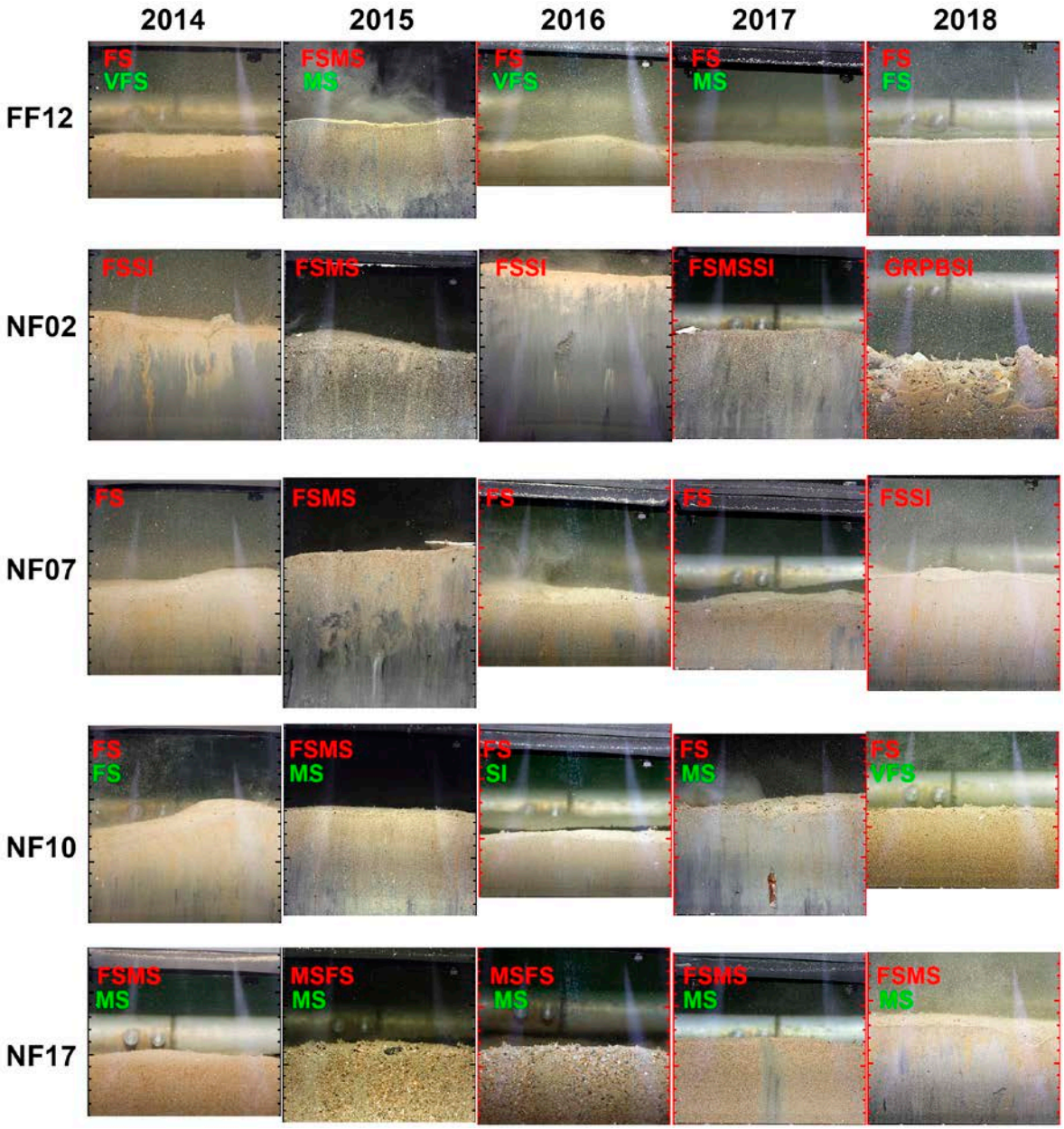

Figure 3-23. Apparent change in modal sediment grain-size at five stations from 2014 to 2018. 2014 was a low storm year, 2016 and 2017 were moderate storm years, and both 2015 and 2018 were high storm years. Modal grain-sizes from SPI analysis are in red. Modal grain-size from sediment analysis are in green. Grain-size descriptors are: FS - fine-sand, GR - gravel, MS - medium-sand, PB - pebble, SI – silt, and VFS – very-fine-sand. Scale on side of images is in cm.

Surficial Sediment Dynamics

In addition to critical erosion threshold and sediment grain-size, biological processes also influence sediment dynamics through biogenic structures that create bed roughness (Solan and Kennedy 2002) and bioturbation that tends to mix sediments (Mermillod-Blondin and Rosenberg 2006). Physical processes would be primarily currents and turbulence, and biological processes primarily organism-sediment-interactions and bioturbation (Rhoads 1974). Processes that shape surficial sediments to create bed roughness can be classified as physical or biological in origin (Thompson et al. 2017). SPI images were visually assessed and assigned to one of three categories (Physical, Biological/Physical, and Biological, see Figure 3-24 for examples). Bed roughness at the majority of nearfield stations was due to combination of physical and biological processes from 1995 to 2005 (Figure 3-25). Biological processes dominated only three years (1998 to 2000) of this interval. Bed roughness at the start of monitoring (1992) and again from 2006 to 2018 was primarily due to physical processes (Figure 3-25).

In addition to the probability of bed roughness being increasingly dominated by physical processes through time (logistic regression, df = 46, Residual Deviance = 733, $p = <0.001$), the probability also increased with increasing integrated stress from winter period storms (df = 44, Residual Deviance = 713, $p = 0.017$). As the annual sum of winter storm stress from IWaveS increased, the predicted probability of physical dominance of bed roughness increased by approximately 0.5 % for every 10 Pa h increase in storm stress and approximately 1.4 % every year (Figure 3-26).

Physical processes dominated at the start of the nearfield SPI monitoring in August 1992, coincident with two of the four largest storms recorded for Massachusetts Bay. These were the October 1991 Perfect Storm (fourth ranked storm for both IWindS and IWaveS) and the Blizzard of 1992 in December 1992 (first for IWindS and second for IWaveS). The highpoint for biological dominance of bed roughness was from 1998 to 2000 when the odds (ratio of biological to physical dominated stations) was over 10 to 1 in favor of biology. These three years saw the longest periods with no major winter storms prior to August monitoring (Figure 3-18). Prior to August 1999 there was a 31-month period with no major IWindS storms and 17-months for IWaveS storms. By 2001, the start of outfall operation, the odds of biological dominance had dropped to less than 2 to 1 (Figure 3-25). Strong winter storms within 5-months of August 2001 were again associated with a steep decline in biological processes. From 2001 on, physical processes started to dominate. For example, in 1998 surficial sediments at station FF13 were biologically dominated, from 1999 to 2001 a combination of physical and biological processes dominated, and from 2002 to 2018 physical processes dominated (Figure 3-24).

The highest annual total number of IWaveS winter storms (24) was in 2015 and was coincident with the highest odds of physical dominance over the monitoring period. In 2016 and 2017, both milder storm years, the odds of physical dominance declined and the odds of biological dominance increased to its highest point since 2002 (Figure 3-27). Physical dominance increased again with a stormy 2018 that had the strongest IWaveS storm (200 Pa h) in March 2018 and the second strongest IWindS storm (45 Pa h) in January 2018.

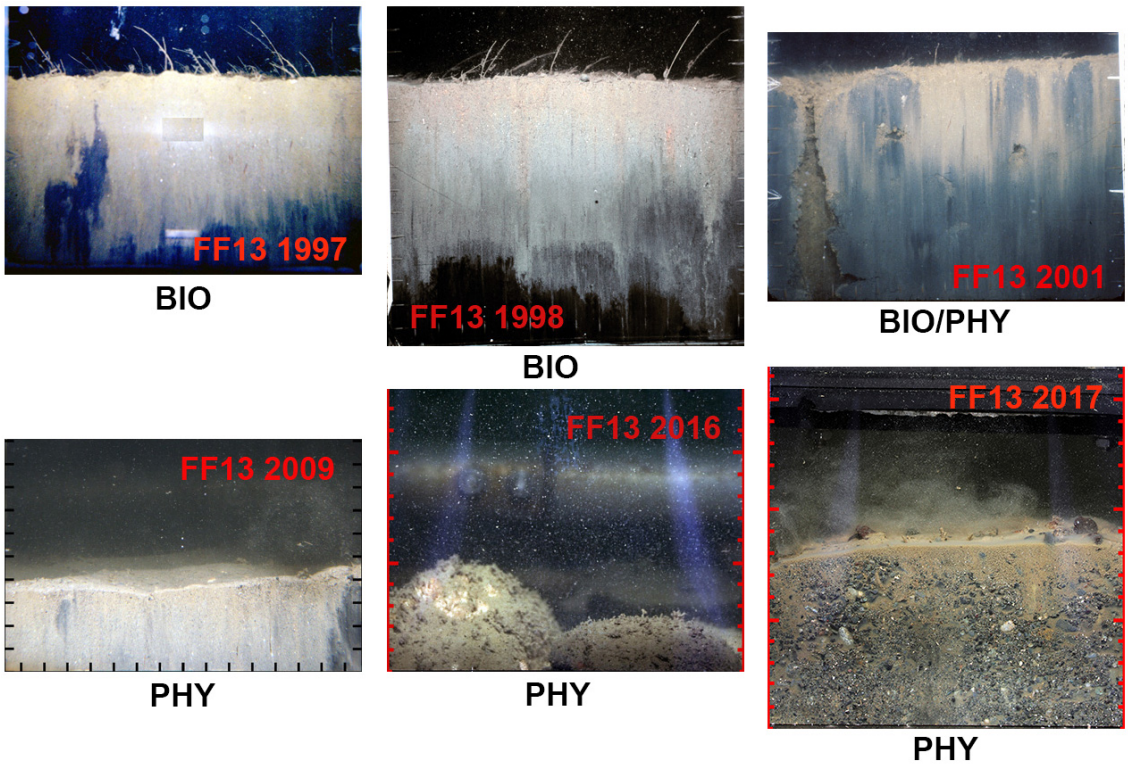

Figure 3-24. Shift in dominance of processes structuring surface sediments at station FF13 through time. BIO = biological dominance, BIO/PHY = combination of biological and physical dominance, PHY = physical dominance. Scale on side of images is in cm.

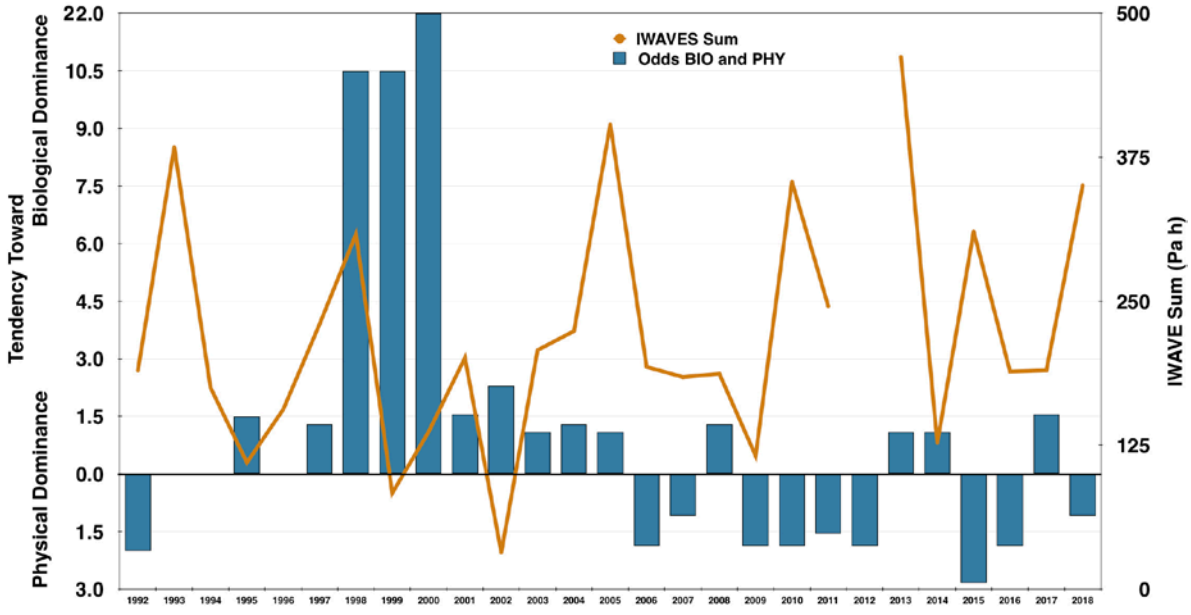

Figure 3-25 Odds of biological verses physical processes dominance of bed roughness for nearfield stations from 1992 to 2018 (bars) and winter period storm intensity measured by integrated bottom-wave stress (IWaveS, line). SPI were not collected in 1993, 1994, or 1996. IWaveS was not calculated for 2012 due to missing data.

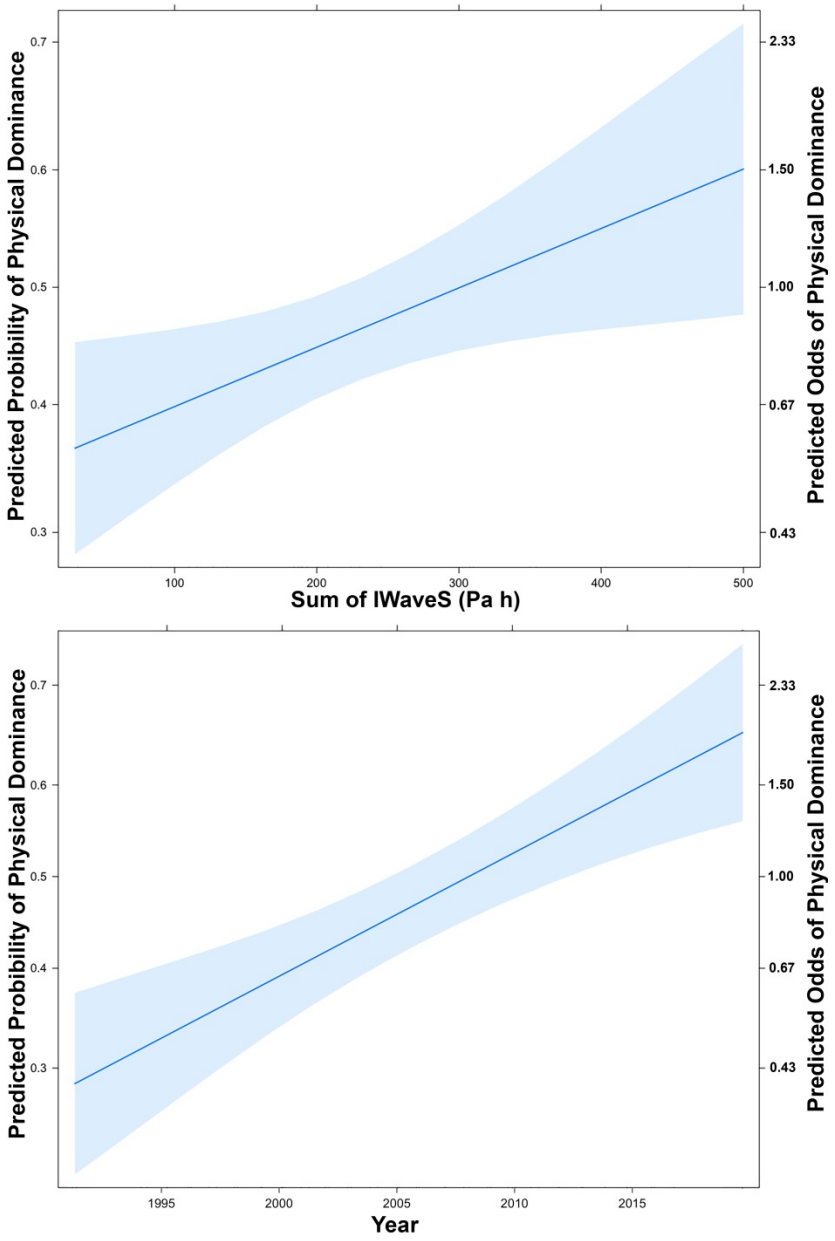

Figure 3-26 Predicted probabilities and odds of physical processes dominating bed roughness for sum of IWaveS and year. Shaded area is 95% confidence interval.

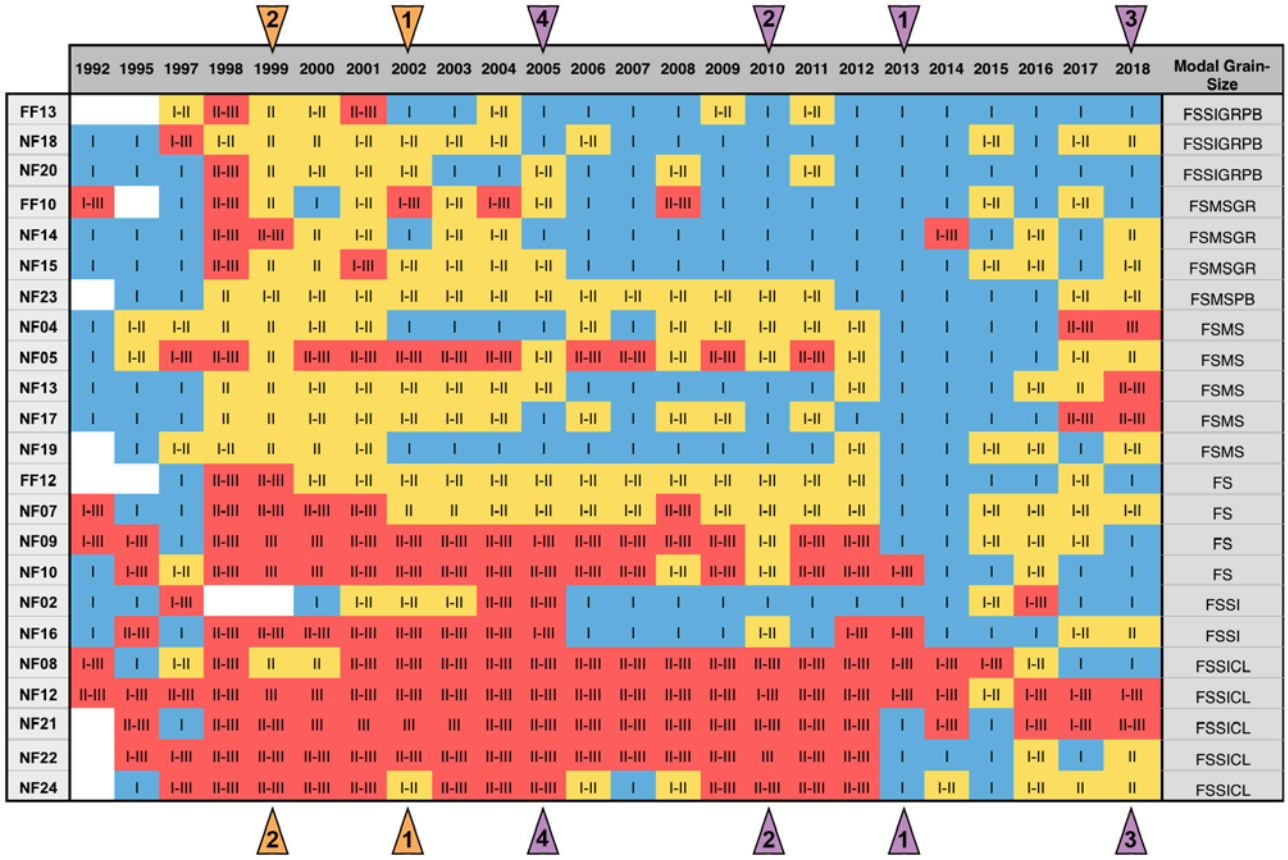

Figure 3-27 Matrix of estimated successional stage for nearfield through time. Stage I is pioneering fauna that is mostly opportunistic species. Stage III is equilibrium fauna that is mostly larger and longer-lived species. Stage II is intermediate to I and III. Top four winter period storm years are purple triangles. Two least stormy years are orange triangles. Stations are ordered by modal grain-size, coarsest to finest. PB is pebble, GR is gravel, MS is medium-sand, FS is fine-sand, SI is silt, and CL is clay.

Biology

The general status of benthic habitat was assessed using the Organism Sediment Index (OSI), biogenic structures, and estimated successional stage (Figure 3-27). From 2004 on, the annual mean OSI indicated good quality benthic habitat (>6) was present across the nearfield. While OSI increased through time, variation in OSI was not related to winter period storms. Most of the increase in OSI was related to deepening of the aRPD layer, a major component of OSI (Rhoads and Germano 1986).

Estimated successional stage, the other major OSI component, over the nearfield was related to storm activity. The largest reduction in successional stage occurred in 2013, the stormiest year between 1991 and 2018 (Figure 3-18), when 11 of 23 stations declined from Stage II or III to Stage I (Figure 3-27). Similar shifts toward Stage I did not occur in 2010, 2018, or 2005, the next three stormiest years.

There was a decrease in the probability and odds of more advanced successional stages (II and III) occurring though time (logistic regression, df = 46, Residual Deviance = 733, p = <0.001; Figures 3-27 and 3-30). Advanced Stage II and III communities dominated from 1998 to 2001 over the nearfield and continued to be dominant up to 2012 at fine-sand-silt-clay stations, and then declined to a low point in 2013 and 2014. Estimated successional stage again increased from 2015 to 2018 (Figure 3-27). Overall, pioneering Stage I, representative of disturbance phase community development (in the sense of Odum 1969), increased though time as Stage II and III declined (Figure 3-28). Disturbance in the case of high-energy environments, like the nearfield, is due primarily to sediment instability that prevents development or persistence of biogenic structures needed by advanced stage fauna. Grouping stations by sediment type, a rough approximation of bottom energy, showed persistence of advanced stage fauna though time in fine-sand-silt-clays, which implies a less energetic bottom (Figure 3-27). At coarse-grained stations, Stages II and III predominated between 1998 and 2004, with Stage I dominating all other years.

The mean number of biogenic structures observed in SPI declined though time (linear regression, df = 1, F = 37.4, p = <0.001; Figure 3-29) along with the occurrence of estimated Stage III fauna. The decline was related to the number of winter period storms but not months since last major storm or sum of IWaveS energy (Table 3-7). For every added winter period storm (when storm intensity and time since last storm are controlled for), the mean number of biogenic structures declined by about 0.4 structures/image.

Similar evaluations were conducted for infauna at the subset of nearfield stations for which infaunal samples are collected (Figure 2-1). Total infaunal abundance declined through time (quasipoisson regression[2], df = 1, Deviance = 1602.5, p = 0.001) but the declining pattern was not related with winter period storms. Similarly, the total number of species (linear regression, df = 1, F = 4.4, p = 0.049) declined, but H' diversity increased (F = 5.4, p = 0.031), through time. Neither was related with winter storms.

While the overall abundance of infauna declined through time and was not related to storms[3], there was a trend for total amphipod and isopod abundance to decline with increasing sum of IWaveS (quasipoisson regression, df = 1, Deviance = 315.6, p = 0.051; Figure 3-30). Life-history traits of amphipods and isopods would make them susceptible to high bottom stress as they tend to live at or just above the sediment-water-interface.

[2] Quasipoisson regression was selected to correct for over-dispersion in the count data. It assumes that the variance is proportional rather than equal to the mean.
[3] As documented in Section 3-2, these infaunal changes, which also occurred at stations distant from the outfall not sampled by the SPI study, show no indication they are related to outfall discharge.

Table 3-7. Analysis of variance from linear regression of winter storm stress (sum of IWaveS), number of storms, and months since the last major storm with the annual mean number of biogenic structures. For every added winter storm, the number of biogenic structures declines by 0.43 structures/image.

	Parameter	SE	z-value	p
Intercept	12.707	3.809	3.34	0.004
Storm Stress	-0.001	0.007	-0.13	0.896
Number of Storms	-0.432	0.191	-2.26	0.038
Months Since Last Major Storm	0.070	0.098	0.10	0.483

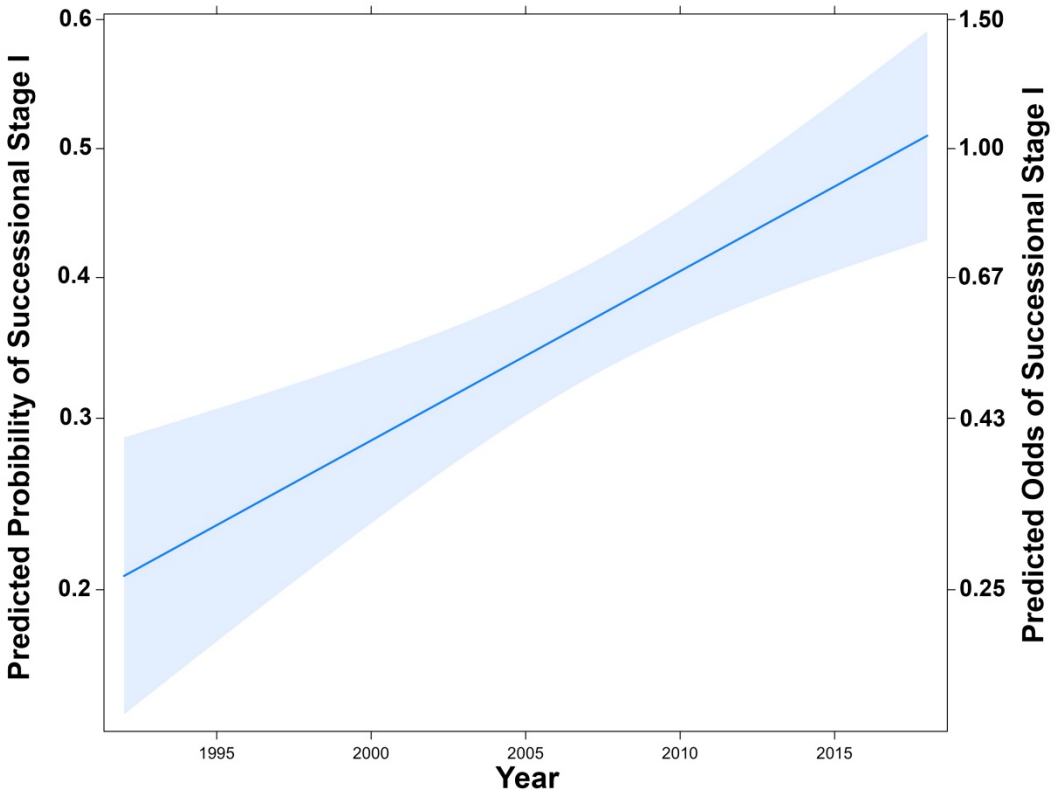

Figure 3-28 Predicted probability and odds of estimated successional Stage I though time. Stage I represents pioneering fauna most with opportunistic life-histories. Shaded area is 95% confidence interval.

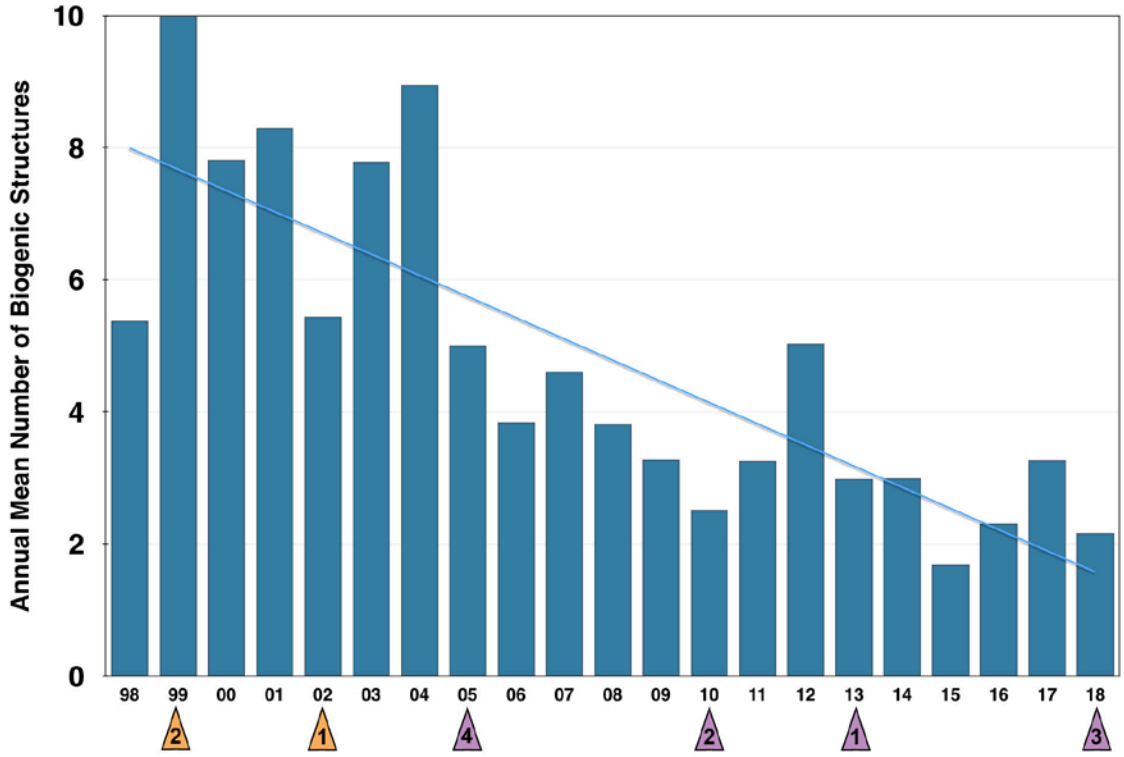

Figure 3-29 Annual mean of total biogenic structures (infauna, burrows, voids) observed in SPI for all 23 nearfield stations. The top four winter period storm years are indicated by purple triangles. The two least stormy years are indicated by orange triangles.

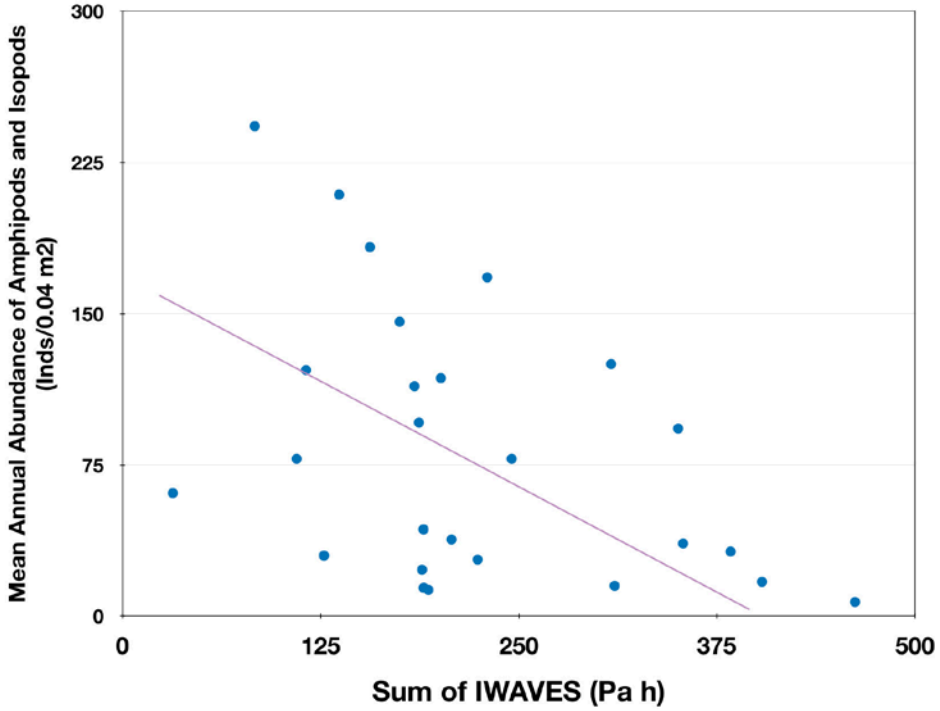

Figure 3-30 Relationship between mean annual abundance of amphipods and isopods with IWaveS. Line is from quasipoisson regression.

Apparent Color Redox-Potential Discontinuity (aRPD) Layer Depth

The grand mean aRPD layer depth in 2018 was among the deepest annual averages for post outfall monitoring and did not exceed the threshold of a 50% decrease from the baseline conditions (Figure 3-31). At 11 of the 23 stations, the aRPD layer was not observed in the SPI images because it was deeper than prism penetration. This was due to either coarse grain-size where pore water circulation oxygenated deeper sediments (Janssen et al. 2005) or high sediment compaction from shell, pebble, or cobble limited prism penetration. If only measured values are considered, the thickness of the aRPD for 2018 would be 4.8 cm (SD = 1.5 cm, 12 stations in mean). A breakpoint linear regression was used to identify patterns in the annual aRPD measurements. From the start of SPI monitoring in 1992 to 2003, the thickness of the annual mean aRPD layer remained unchanged with an average of 2.2 cm over this period (R^2 = <0.01, p = 0.980). From 2004 to 2013 the aRPD layer depth was variable but trended deeper by about 0.2 cm per year (R^2 = 0.59, p = 0.010). Starting in 2014 the aRPD layer depth remained the same through to 2018 (R^2 = 0.13, p = 0.545; Figure 3-31) and averaged 4.8 cm.

The general nearfield pattern of increasing aRPD depth through time could be seen at five fine-sand-silt-clay sediment stations (NF08, NF12, NF21, NF22, NF24) with measured aRPD layers from 1997 through 2018 (Figure 3-32). From 2012 to 2016 the aRPD layer was consistently above the long-term averages for these stations. In 2017, aRPD layers at Stations NF08 and NF12 declined below the long-term average. In 2018, Station NF24 had the greatest increase in aRPD followed by NF08. The other three stations declined (Figure 3-32).

The deepening of the aRPD layer through time along with a general increase in OSI starting in 2004 (breakpoint linear regression R^2 = 0.45, p = 0.004; Figure 3-33) indicated the presence of high quality benthic habitat in the nearfield. Community structure and high diversity of benthos also confirms the presence of high quality benthic habitat (see Section 3.2). Had outfall operation degraded benthic habitat quality both aRPD layer depth and diversity would have declined, as has been observed at other ocean outfalls (Puente and Diaz 2015).

Nearfield Summary

There continues to be no evidence of an outfall effect on infaunal benthic habitat quality based on sediment profile imaging (SPI) data for 2018. In comparing baseline habitat conditions (1992 to 2000) with post-baseline outfall operation conditions (2001 to 2018) there have not been any changes in benthic habitat quality that can be attributed to outfall operation. Changes that have occurred are regional and related primarily to storm intensity and frequency, and secondarily to temporal trends.

The processes structuring surficial sediments in the nearfield appeared to be related primarily to the intensity and number of major storm events, and secondarily to the timing of storms prior to the annual August SPI sampling (Figure 3-18). Storms appeared to affect the entire nearfield region. Strongest relationships were with medium to coarse grained sediment stations. Finer grained stations tended to have no or weaker associations with storms.

The dominance of hydrodynamic and physical factors in the nearfield was related to storm events with their associated bottom stresses and currents, turbulence, and sediment transport (Butman et al. 2008).

These are the principal reasons that benthic habitat quality in the nearfield is not associated with outfall operation. The high-energy environment in the region of the outfall disperses effluents quickly and prevents degradation of soft bottom benthic infaunal habitat. The lack of accumulation of organic matter in the sediments is the principle reason for lack of benthic impacts. In general, coastal ocean sewage outfalls with low or no detectable impacts in benthic infauna based on SPI and community analyses appeared to be related to low accumulation rates for organic matter and dominance of high energy physical processes (Puente and Diaz 2015).

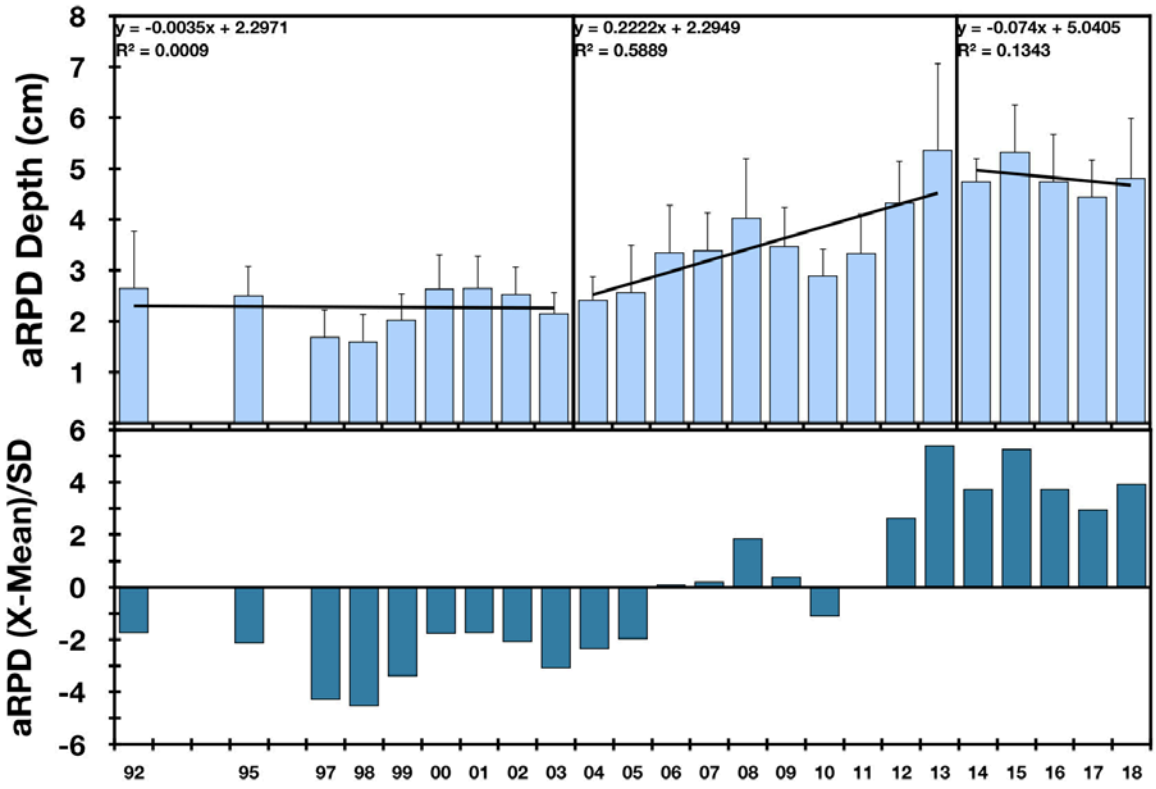

Figure 3-31 Average annual aRPD layer depth for nearfield stations with measured aRPD layers. Bars are one standard deviation. Lines are based on breakpoint linear regression. Lower panel is pattern of standardized (mean centered and unit variance) aRPD layer depths.

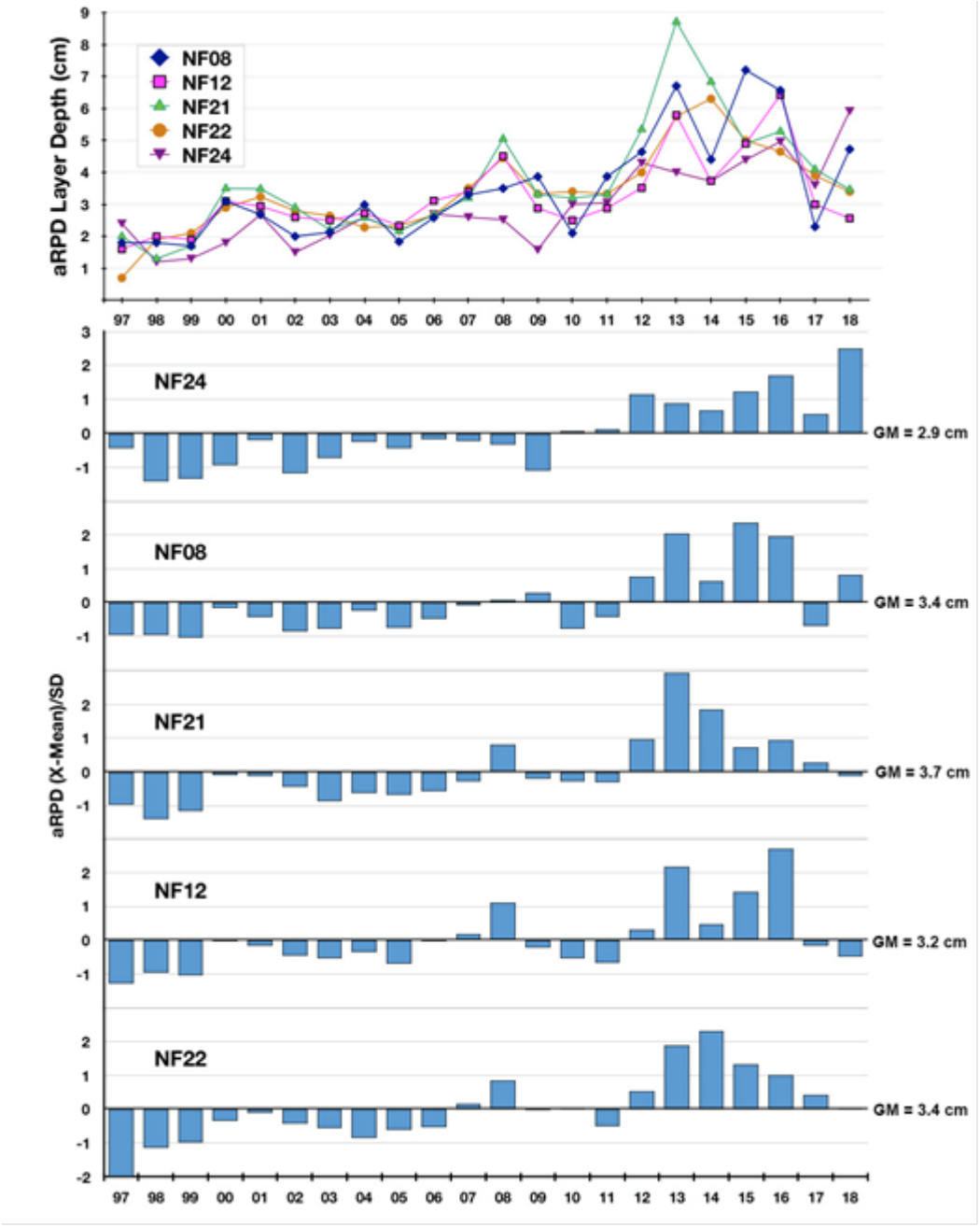

Figure 3-32 Pattern in aRPD layer depth from 1997 to 2018 at stations with measured aRPD every year. The aRPD layer grand mean (for all years) for each station is shown to the right.

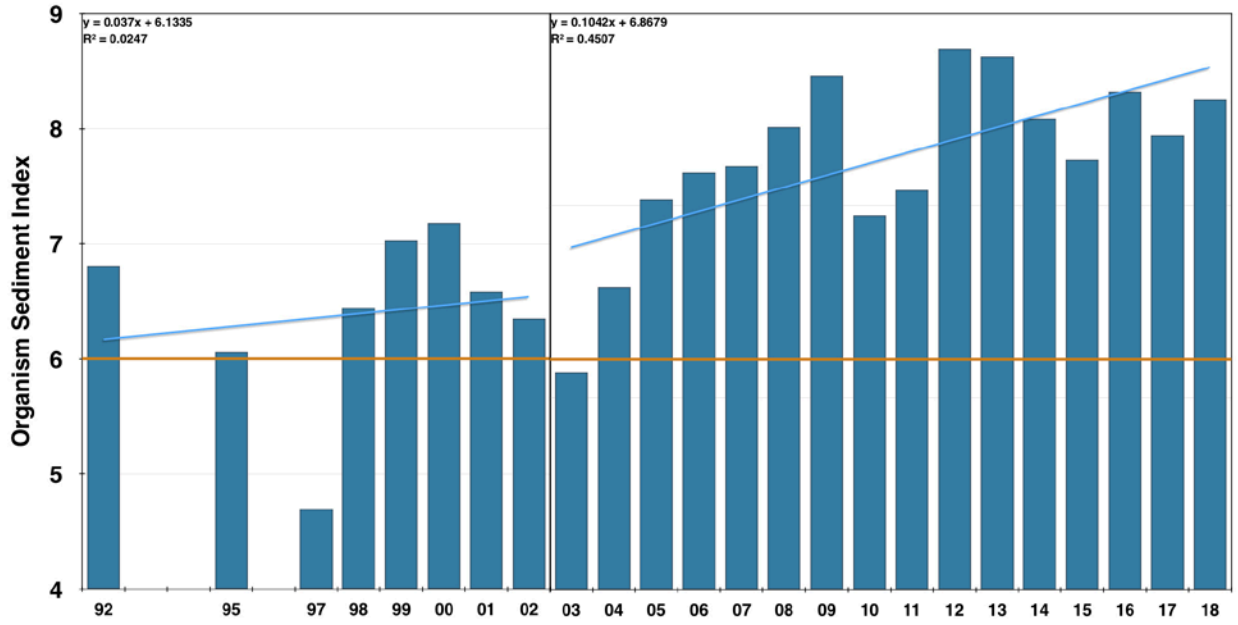

Figure 3-33 Average annual Organism Sediment Index (OSI) at nearfield stations. Regression lines are based on breakpoint linear regression. OSI values >6 represent good benthic habitat conditions (Rhoads and Germano 1986).

4 SUMMARY OF RELEVANCE TO MONITORING OBJECTIVES

Benthic monitoring for MWRA's offshore ocean outfall focused on addressing three primary concerns regarding potential impacts to the benthos from the wastewater discharge: (1) eutrophication and related low levels of dissolved oxygen; (2) accumulation of toxic contaminants in depositional areas; and (3) smothering of animals by particulate matter.

Results of the SPI survey provide important insight into the question of eutrophication and dissolved oxygen. As has been noted throughout the post-diversion period, the 2018 SPI survey continued to find no indication that the wastewater discharge has resulted in lower levels of dissolved oxygen in nearfield sediments. The average thickness of the sediment oxic layer in 2018 was greater than reported during the baseline period. The SPI results continued to suggest a trend towards a predominance of a pioneering stage benthic community, a result indicative of increases in physical (storm-related) stress on the community. There is no evidence that the source of this stress is organic pollution; for example the infaunal study found that the numbers of opportunistic species remained negligible in 2018. The source of stress appears to be associated with storms in Massachusetts Bay that cause resuspension of bottom sediments.

This report includes an assessment of regional storminess since sediment monitoring began in 1992, and the potential for those storms to impact the benthos. This assessment strongly supports that the trend seen in the SPI survey likely results from the coarsening of sediment grain-size caused by sediment mixing and transport associated with storms that caused a decline in visible biogenic structures in the images. These results support previous findings that eutrophication and the associated decrease in oxygen levels have not been a problem at the nearfield benthic monitoring stations (Nestler et al. 2018, Maciolek et al. 2008). The outfall is located in an area dominated by hydrodynamic and physical factors, including tidal and storm currents, turbulence, and sediment transport (Butman et al. 2008). Storm events significant enough to impact bottom sediments in Massachusetts Bay are common events. Further, there is substantial evidence that storm impacts on nearfield sediments and benthos may have increased since the start of monitoring. These physical factors, along with the high quality of the effluent discharged into the Bay (Taylor 2010), are the principal reasons that benthic habitat quality has remained high in the nearfield area.

Surveys of soft-bottom benthic communities continue to suggest that animals near the outfall have not been smothered by particulate matter from the wastewater discharge. The percentage of fine grain sediments has not increased in the nearfield stations since the diversion indicating no substantial settlement of particulate matter from the discharge. There were no Contingency Plan threshold exceedances for any infaunal diversity measures in 2018.

Benthic monitoring results continued to indicate that the three potential impacts of primary concern (decreased oxygen; accumulation of contaminants; and particulate deposition that smothers the benthos) have not occurred at the MWRA stations. Results also continue to demonstrate that the benthic monitoring program comprises a sensitive suite of parameters that can detect both the influence of the outfall and the subtle natural changes in benthic communities. The spatial extent of particulate deposition from the wastewater discharge is measurable in the *Clostridium perfringens* concentrations in nearfield

sediments. *C. perfringens* concentrations provide evidence of the discharge footprint at stations close to the outfall. Within this footprint, no other changes to sediment composition and infaunal communities have been detected. Nonetheless, subtle variations in the species composition of infaunal assemblages clearly delineate natural spatial variation in the benthic community based on habitat (e.g., associated with different sediment grain sizes) and bottom energy (e.g., turbulence and sediment transport associated with storm events). Changes over time have also been detected including a region-wide shift towards higher diversity and lower dominance in the Massachusetts Bay infaunal assemblages. Detection of these spatial and temporal patterns in the benthos suggests that any ecologically significant adverse impacts from the outfall would be readily detected by the monitoring program, if those impacts had occurred.

5 REFERENCES

Agresti A. 1990. Categorical data analysis. New York: Wiley. 558 p.

Bothner MH, Casso MA, Rendigs RR, Lamothe PJ. 2002. The effect of the new Massachusetts Bay sewage outfall on the concentrations of metals and bacterial spores in nearby bottom and suspended sediments. Marine Pollution Bulletin. 44: 1063-1070.

Butman B, Sherwood CR, Dalyander PS. 2008. Northeast storms ranked by wind stress and wave-generated bottom stress observed in Massachusetts Bay, 1990–2006. Continental Shelf Research 28:1231–1245.

Chapman PM, Paine MD, Arthur AD, Taylor LA. 1996. A triad study of sediment quality associated with a major, relatively untreated marine sewage discharge. Marine Pollution Bulletin 32:47-64.

Clarke KR. 1993. Non-parametric multivariate analyses of changes in community structure. Aust. J. Ecol., 18: 117-143.

Clarke KR, Green RH. 1988. Statistical design and analysis for a 'biological effects' study. Mar. Ecol. Prog. Ser., 46: 213-226.

Constantino J, Leo W, Delaney MF, Epelman P, Rhode S. 2014. Quality assurance project plan (QAPP) for sediment chemistry analyses for harbor and outfall monitoring, Revision 4 (February 2014). Boston: Massachusetts Water Resources Authority. Report 2014-02. 53 p.

Diaz RJ, Rhoads DC, Blake JA, Kropp RK, Keay KE. 2008. Long-term trends in benthic habitats related to reduction in wastewater discharges to Boston Harbor. Estuaries and Coasts 31:118–1197.

Elías R, Palacios JR, Rivero MS, Vallarino EA. 2005. Short-term responses to sewage discharge and storms of subtidal sand-bottom macrozoobenthic assemblages off Mar del Plata City, Argentina (SW Atlantic). Journal of Sea Research 53:231-42.

Janssen F, Huettel M, Witte U. 2005. Pore-water advection and solute fluxes in permeable marine sediments (II): Benthic respiration at three sandy sites with different permeabilities (German Bight, North Sea). Limnology and Oceanography 50:779-792.

Maciolek NJ, Diaz RJ, Dahlen DT, Hecker B, Williams IP, Hunt CD, Smith WK. 2007. 2006 Outfall benthic monitoring report. Boston: Massachusetts Water Resources Authority. Report 2007-08. 162 p.

Maciolek NJ, Doner SA, Diaz RJ, Dahlen DT, Hecker B, Williams IP, Hunt CD, Smith W. 2008. Outfall Benthic Monitoring Interpretive Report 1992–2007. Boston: Massachusetts Water Resources Authority. Report 2008-20. 149 p.

Mermillod-Blondin F, Rosenberg R. 2006. Ecosystem engineering: the impact of bioturbation on biogeochemical processes in marine and freshwater benthic habitats. Aquatic Sciences 68:434-442.

MWRA. 1991. Massachusetts Water Resources Authority effluent outfall monitoring plan phase I: baseline studies. Boston: Massachusetts Water Resources Authority. Report 1991-ms-02. 95 p.

MWRA. 1997. Massachusetts Water Resources Authority Contingency Plan. Boston: Massachusetts Water Resources Authority. Report 1997-ms-69. 41 p.

MWRA. 2001. Massachusetts Water Resources Authority Contingency Plan Revision 1. Boston: Massachusetts Water Resources Authority. Report ENQUAD ms-071. 47 p.

MWRA. 2004. Massachusetts Water Resources Authority Effluent Outfall Ambient Monitoring Plan Revision 1, March 2004. Boston: Massachusetts Water Resources Authority. Report 1-ms-092. 65 p.

MWRA. 2010. Ambient monitoring plan for the Massachusetts Water Resources Authority effluent outfall revision 2. July 2010. Boston: Massachusetts Water Resources Authority. Report 2010-04. 107p.

Nestler EC, Diaz RJ, Hecker B. 2018. Outfall Benthic Monitoring Report: 2017 Results. Boston: Massachusetts Water Resources Authority. Report 2018-05. 57 p. plus Appendices.

Nestler EC, Diaz RJ, Pembroke AE. 2017. Outfall Benthic Monitoring Report: 2016 Results. Boston: Massachusetts Water Resources Authority. Report 2017-08. 37 p. plus Appendices.

Odum EP. 1969. The strategy of ecosystem development. Science 164:262-270.

Puente A, Diaz RJ. 2015. Response of benthos to ocean outfall discharges: does a general pattern exist? Marine Pollution Bulletin 101:174-81.

Rhoads DC. 1974. Organism sediment relations on the muddy sea floor. Oceanography and Marine Biology Annual Review 12:263-300.

Rhoads DC, Germano JD. 1986. Interpreting long-term changes in benthic community structure: A new protocol. Hydrobiologia 142:291-308.

Rutecki DA, Nestler EC, Hasevlat RC. 2017. Quality Assurance Project Plan for Benthic Monitoring 2017–2020. Boston: Massachusetts Water Resources Authority. Report 2017-06, 92 p. plus Appendices.

Signell RP, Jenter HL, Blumberg AF. 2000. Predicting the physical effects of relocating Boston's sewage outfall. Estuarine, Coastal and Shelf Science 50:59-71.

Solan M, Kennedy R. 2002. Observation and quantification of in situ animal-sediment relations using time-lapse sediment profile imagery (t-SPI). Marine Ecology Progress Series 228:179-191.

Taylor DI. 2010. The Boston Harbor Project, and large decreases in loadings of eutrophication-related materials to Boston Harbor. Marine Pollution Bulletin 60:609–619.

Thompson CEL, Williams ME, Amoudry L, Hull T, Reynolds S, Panton A, Fones GR. 2017. Benthic controls of resuspension in UK shelf seas: implications for resuspension frequency. Continental Shelf Research. (doi:10.1016/j.csr.2017.12.005).

Warner JC, Butman B, Dalyander PS. 2008. Storm-driven sediment transport in Massachusetts Bay. Continental Shelf Research 28:257-282.

Warwick RM. 1993. Environmental impact studies on marine communities: pragmatical considerations. Aust. J. Ecol., 18: 63-80.

Massachusetts Water Resources Authority
100 First Avenue • Boston, MA 02129
www.mwra.com
617-242-6000